

Stereoselective Alcohol Silylation by Dehydrogenative Si–O Coupling: Scope, Limitations, and Mechanism of the Cu–H-Catalyzed Non-Enzymatic Kinetic Resolution with Silicon-Stereogenic Silanes

Sebastian Rendler,^[a, b] Oliver Plefka,^[b] Betül Karatas,^[a] Gertrud Auer,^[b] Roland Fröhlich,^[a] Christian Mück-Lichtenfeld,^[c] Stefan Grimme,^[c] and Martin Oestreich*^[a, b]

Abstract: Ligand-stabilized copper(I)–hydride catalyzes the dehydrogenative Si–O coupling of alcohols and silanes—a process that was found to proceed without racemization at the silicon atom if asymmetrically substituted. The present investigation starts from this pivotal observation since silicon-stereogenic silanes are thereby suitable for the reagent-controlled kinetic resolution of racemic alcohols, in which asymmetry at the silicon atom enables discrimination of enantiomeric alcohols. In this full account, we summarize

our efforts to systematically examine this unusual strategy of diastereoselective alcohol silylation. Ligand (sufficient reactivity with moderately electron-rich monophosphines), silane (reasonable diastereocontrol with cyclic silanes having a distinct substitution pattern) as well as substrate identification (chelating donor as a requirement) are

introducerily described. With these basic data at hand, the substrate scope was defined employing enantiomerically enriched *tert*-butyl-substituted 1-silatetraline and highly reactive 1-silaindane. The synthetic part is complemented by the determination of the stereochemical course at the silicon atom in the Si–O coupling step followed by its quantum-chemical analysis thus providing a solid mechanistic picture of this remarkable transformation.

Keywords: alcohols • asymmetric catalysis • copper • kinetic resolution • silicon

Introduction

The Si–O linkage is an attractive connectivity for synthetic organic chemists. On the one hand, the strong Si–O bond ensures its compatibility with the majority of synthetic methods and, on the other hand, the availability of orthogonal strategies for (chemo)selective bond formation and cleavage account for the extensive utilization of silyl ethers to temporarily protect hydroxy groups in complex molecule synthesis.^[1] For these reasons, the development of stereoselective alcohol silylation methodology is of considerable interest. Such strategies would substantially increase the value of silyl ether formation and, thus, complement existing asymmetric carbonyl hydrosilylation techniques.^[2]

Following a report by Ishikawa and co-workers,^[3] stereoselective alcohol silylation has increasingly attracted attention in recent years.^[4] We and, shortly thereafter, Hoveyda and Snapper et al. devised fundamentally different concepts for stereoselective Si–O coupling.^[5,6] From a synthetic perspective, both approaches constitute novel strategies for non-enzymatic kinetic resolution of racemic mixtures of al-

[a] Dr. S. Rendler, Dr. B. Karatas, Dr. R. Fröhlich,⁺ Prof. Dr. M. Oestreich
Organisch-Chemisches Institut
Westfälische Wilhelms-Universität Münster
Corrensstrasse 40, 48149 Münster (Germany)
Fax: (+49)251-83-36501
E-mail: martin.oestreich@uni-muenster.de

[b] Dr. S. Rendler, Dipl.-Chem. O. Plefka, Dr. G. Auer,
Prof. Dr. M. Oestreich
Institut für Organische Chemie und Biochemie
Albert-Ludwigs-Universität Freiburg
Albertstrasse 21, 79104 Freiburg im Breisgau (Germany)

[c] Dr. C. Mück-Lichtenfeld, Prof. Dr. S. Grimme
Theoretische Organische Chemie
Organisch-Chemisches Institut
Westfälische Wilhelms-Universität Münster
Corrensstrasse 40, 48149 Münster (Germany)
E-mail: grimmes@uni-muenster.de

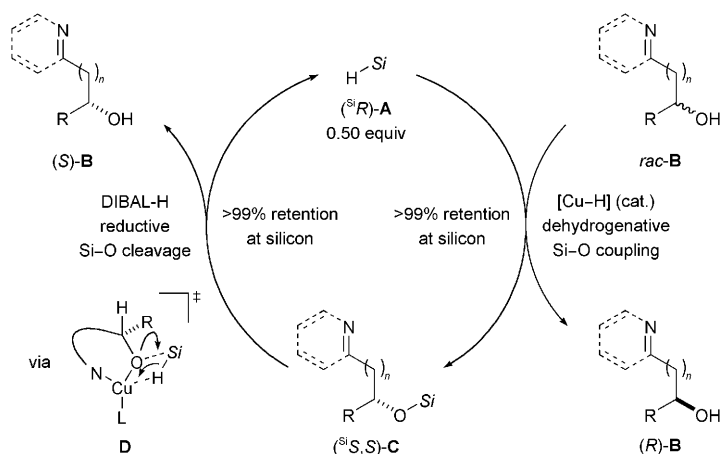
[⁺] X-ray crystal structure analysis.

Supporting information for this article is available on the WWW under <http://dx.doi.org/10.1002/chem.200801377>.

cohols^[7] or desymmetrization of *meso* diols,^[8] respectively, an area, in which asymmetric acylation^[9] has been the prevailing methodology thus far. Our strategy for kinetic resolution of racemic alcohols relies on a reagent-controlled, congruently diastereoselective, dehydrogenative Si–O coupling^[10,11] with recyclable silicon-stereogenic silanes (Scheme 1).^[5] In this process, a transition-metal hydride, for

at the silicon atom facilitated promising stereoselectivity in kinetic resolution of secondary alcohols.

In this full account, we present a comprehensive investigation of the factors governing the stereoselectivity in the ki-



Scheme 1. Cu–H-catalyzed diastereoselective alcohol silylation: Kinetic resolution with recyclable silicon-stereogenic silanes. *Si* represents an asymmetrically substituted silicon atom.

example, ligand-stabilized copper(I) hydride,^[12] facilitates a diastereodiscriminating reaction of enantiopure chiral silane (^{Si}*R*)-**A** with one out of two possible enantiomers of a donor-functionalized chiral alcohol *rac*-**B** to form silyl ether (^{Si}*S,S*)-**C**. Notably, dihydrogen is formed as the sole by-product.^[13] Along with diastereoenriched silyl ether (^{Si}*S,S*)-**C**, the slow-reacting enantiomer of the alcohol (*R*)-**B** remains in enantioenriched form. As delineated in the assumed transition state **D**, σ -bond metathesis of a copper(I) alkoxide with the silane might account for diastereoselective Si–O coupling.^[14] The virtue of σ -bond metathesis for enantiospecific transformations of silicon-stereogenic silanes (retention of configuration is observed) had already been disclosed in earlier contributions by our group.^[15,16] Two-point binding by coordination of the pending donor in the substrate was shown to be essential in order to achieve good diastereoselectivity. A second synthetic operation then completes the concept: Enantiospecific reductive cleavage^[17] of the Si–O bond with DIBAL-H liberates the resolving reagent (^{Si}*R*)-**A** along with alcohol (*S*)-**B** [(^{Si}*S,S*)-**C** \rightarrow (^{Si}*R*)-**A**].^[5a]

Our initial studies^[5a,15a,16c] also underlined the importance of the substitution pattern at silicon in order to achieve useful levels of diastereoinduction in the Si–O coupling event. Acyclic triorganosilanes such as (^{Si}*R*)-**1**^[18] and (^{Si}*R*)-**2**^[19] as well as silatetraline (^{Si}*R*)-**3**^[20a] invariably showed insufficient reagent control. From these insights, silane (^{Si}*R*)-**4a**^[20b] emerged as the reagent of choice (see Figure 1). Embedded into a rigid cyclic framework and equipped with three substituents of different steric demand, the asymmetry

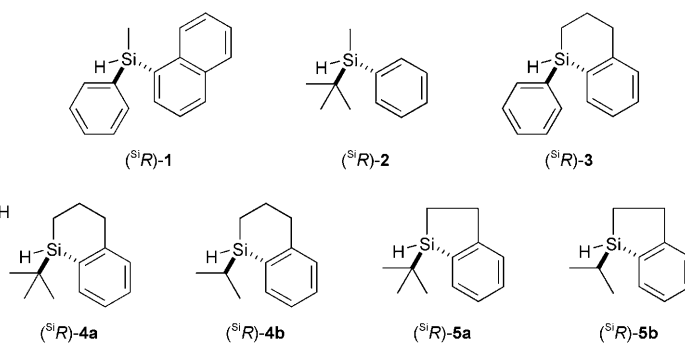


Figure 1. Silicon-stereogenic silanes for kinetic resolution of secondary alcohols.

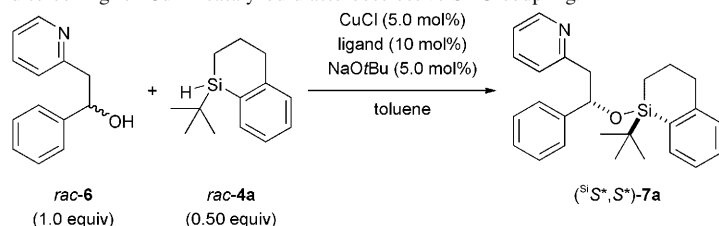
netic resolution of secondary donor-functionalized alcohols by Cu–H-catalyzed dehydrogenative Si–O coupling. A more refined ligand screening, the influence of the tether length in the donor-functionalized alcohol, and structural features of the resolving silane are investigated. Subsequently, the substrate scope with regard to both substituents and the donor is included; results of the kinetic resolution with highly reactive 1-silaindane (^{Si}*R*)-**5a** are discussed as well. A quantum-chemical investigation combined with experimental data on the stereochemical course of the Si–O coupling step gives mechanistic insight into this copper(I) catalysis.

Results and Discussion

Parameters influencing diastereocontrol: At the initial stages of this project, the reaction setup of the Cu–H-catalyzed dehydrogenative Si–O coupling^[13] involved standard substrate *rac*-**6**, silane *rac*-**4a**, and a catalyst generated in situ as reported earlier by Buchwald^[14] and Leighton^[21] [*rac*-**6** \rightarrow (^{Si}*S**,*S**)-**7a**, Table 1]. As an advantage of the reagent-controlled nature of this process, all optimization experiments were conducted with readily available racemic silane; determination of the diastereomeric ratio of the formed silyl ether **7a** by ¹H NMR spectroscopy was sufficiently accurate. Importantly, the diastereomeric excess, which is independent of the degree of conversion in the racemic case, correlates directly with the enantiomeric excess of the slow-reacting alcohol at exactly 50% conversion in a hypothetical kinetic resolution with enantiopure silane.^[22]

Catalyst optimization by ligand screening: In previous studies, monodentate triarylphosphines were identified as the ligands of choice in order to form copper(I) complexes that combine sufficient reactivity with reasonable diastereoselectivity.^[5a] The results compiled in Table 1 give a more refined picture for this ligand class. Compared to parent Ph₃P (**L1a**)

Table 1. Ligand screening for Cu–H-catalyzed diastereoselective Si–O coupling.^[a]



Entry	Ligand L	L/CuCl	t [h]	T [°C]	Conv [%] ^[b]	d.r. ^[c]
1	Ph ₃ P (L1a)	2:1	48	20	42	90:10
2	(4-MeC ₆ H ₄) ₃ P (L1b)	2:1	9	20	38	92:8
3	(4- <i>t</i> BuC ₆ H ₄) ₃ P (L1c)	2:1	8	20	48	88:12
4	(3,5-xylyl) ₃ P (L1d)	2:1	20	20	50	92:8
5	(4-F ₃ CC ₆ H ₄) ₃ P (L1e)	2:1	60	70	38	83:17
6	[3,5-(F ₃ C) ₂ C ₆ H ₃] ₃ P (L1f)	2:1	60	70	34	86:14
7	[4-(MeO)C ₆ H ₄] ₃ P (L1g)	2:1	13	20	33	91:9
8	<i>t</i> BuPh ₂ P (L2)	2:1	16	45	50	90:10
9 ^[d]	IMes-HCl (L3a)	1:1	2	60	40	76:14
10 ^[d]	IPr-HCl (L3b)	1:1	2	85	10	55:45

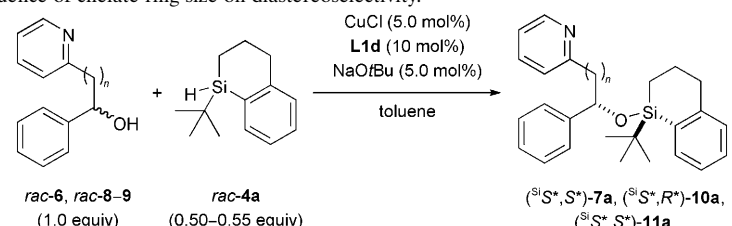
[a] Unless otherwise noted, all reactions were conducted using CuCl (5.0 mol%), the indicated ligand (10 mol% for **L1** and **L2**, 5.0 mol% for **L3**), and NaOtBu (5.0 mol%) with a substrate concentration of 0.1 M in toluene at the indicated temperature. [b] Monitored by ¹H NMR spectroscopy and determined by integration of baseline-separated resonance signals of **6** at δ = 5.18 ppm and **7a** at δ = 4.96/5.05 ppm. [c] Determined by ¹H NMR spectroscopy of the crude reaction mixture by integration of baseline-separated resonance signals of (Si,S*,S*)-**7a** at δ = 4.96 and (Si,S*,R*)-**7a** at δ = 5.05 ppm. [d] Substoichiometric amounts of NaOtBu (30 mol%) used. IMes = 1,3-bis(2,4,6-trimethylphenyl)imidazol-2-ylidene, IPr = 1,3-bis(2,6-diisopropylphenyl)imidazol-2-ylidene.

(entry 1), alkyl substitution on the aromatic rings had only minor effect on diastereoselectivity but considerably improved conversion; slightly more electron-rich phosphines **L1b**, **L1c** and **L1d** (entries 2–4) all resulted in smooth conversion at room temperature. In particular, (3,5-xylyl)₃P (**L1d**) led to complete conversion within 20 h along with the highest diastereoselectivity observed (d.r. 92:8) (entry 4). Conversely, electron-withdrawing groups at the arenes resulted in significantly diminished reactivity; only partial conversion at elevated temperatures was achieved with trifluoromethyl-substituted ligands **L1e** and **L1f** (entries 5 and 6). In contrast, phosphine **L1g** equipped with an electron-rich aromatic ring formed a reactive and selective yet unstable catalyst, that decomposed before conversion of silane **rac-4a** was complete (entry 7). We also considered the use of commercially available, bulky diarylalkylphosphine **L2** (entry 8). As opposed to disappointing results with Buchwald-type ligands as well as trialkylphosphines,^[5a] **L2** showed good reactivity and appreciable diastereoselectivity. The poor diastereoselectivities obtained with *N*-heterocyclic carbene ligands **L3a** and **L3b** (entries 9 and 10) contrast with our recent findings for the related rhodium(I)-catalyzed protocol;^[5a,c] this might indicate different coordination spheres of the transition metals (Cu^I tetrahedral versus Rh^I square-planar).

Chelate ring size: With the catalyst system consisting of CuCl, **L1d** and NaOtBu at hand, we next turned our attention to the tether length between the hydroxy oxygen and

the donor site (Table 2). For this, *rac-6* (*n* = 1, entry 2) was compared with pyridyl methanol *rac-8* (*n* = 0, entry 1) and pyridyl propanol *rac-9* (*n* = 2, entry 3). Not surprisingly, *rac-8*—likely to involve a five-membered chelate ring—also underwent the desired Si–O coupling to give silyl ether (Si,S*,R*)-**10a** (*n* = 0) in markedly decreased diastereoselectivity (d.r. 81:19, entry 1). A pronounced effect on both reactivity and diastereoselectivity was seen in the dehydrogenative coupling of *rac-9* (*n* = 2, d.r. 79:21, entry 3); it reacted only sluggishly at elevated temperatures and prolonged reaction times [*rac-9* → (Si,S*,S*)-**11a**]. An entropically disfavored seven-membered chelate might account for this. Yet, a temporary copper(I)–nitrogen interaction is nevertheless likely since the observed diastereoselectivity is still significantly higher than for a related alcohol devoid of a pending donor; 1,2-diphenyl ethanol gave a 60:40 mixture of diastereomers.^[5a]

Silane-substitution pattern: The distinct influence of the silane design in this kinetic resolution is evident from a mechanistic perspective: The silicon atom as the sole source of stereochemical information is responsible for enantiodiscrimination between the enantiomeric copper(I) alkoxide complexes (cf. **D**, Scheme 1). In order to identify silane lead structures, a broad selection of chiral silanes was surveyed (Table 3). Attempts to utilize known chiral silanes, for example, Sommer's acyclic *rac-1*,^[18] were hampered by the inadequate design for the present purpose with the diastereoselection in the reaction with *rac-6* not exceeding 57:43 [*rac-6* → (Si,S*,S*)-**12**, Table 3, entry 1].^[5a] While in this case poor diastereoselectivity might be attributed to insufficient steric differentiation of the three substituents at silicon, phenyl and 1-naphthyl are similar, such arguments do not hold true for acyclic congener *rac-2*^[19b] [*rac-6* → (Si,S*,S*)-**13**, entry 2];^[16c] low diastereocontrol in the formation of (Si,S*,S*)-**13** is in sharp contrast to its successful utilization in a highly diastereoselective palladium(II)-catalyzed hydrosilylation.^[16c,d] Incorporating the stereogenic silicon center into a rigid cyclic framework provided a solution to this dilemma; however, silatetraline *rac-3*^[20a] equipped with an exocyclic phenyl group performed almost as poor as any of the acyclic reagents [*rac-6* → (Si,S*,S*)-**14**, entry 3].^[5a] We reasoned that, again, insufficient steric differentiation of substituents, phenyl versus phenyl in back-bone, might account

Table 2. Influence of chelate ring size on diastereoselectivity.^[a]


Entry	Alcohol	<i>t</i> [h]	<i>T</i> [°C]	Conv [%] ^[b]	Silyl ether	Yield [%] ^[c]	d.r. ^[d]
1	<i>rac-8</i> (<i>n</i> =0)	24	20	50 ^[e]	(^{Si} <i>S</i> *, <i>R</i> *)- 10a (<i>n</i> =0)	37 (43)	81:19
2	<i>rac-6</i> (<i>n</i> =1)	20	20	47 ^[f]	(^{Si} <i>S</i> *, <i>S</i> *)- 7a (<i>n</i> =1)	44 (50)	92:8
3	<i>rac-9</i> (<i>n</i> =2)	62	50	45 ^[f]	(^{Si} <i>S</i> *, <i>S</i> *)- 11a (<i>n</i> =2)	34 (40)	79:21

[a] All reactions were conducted using CuCl (5.0 mol%), ligand **L1d** (10 mol%), and NaOtBu (5.0 mol%) with a substrate concentration of 0.1 M in toluene at the indicated temperature. [b] Monitored by ¹H NMR spectroscopy and determined by integration of baseline-separated resonance signals. [c] Isolated yield of analytically pure material after flash chromatography; numbers in parentheses refer to reisolated alcohol. [d] Determined by ¹H NMR spectroscopy of the crude reaction mixture by integration of baseline-separated resonance signals of the diastereomers. [e] 0.50 equiv of *rac-4a* used. [f] 0.55 equiv of *rac-4a* used.

for this outcome. This finally led to the design of privileged silane *rac-4a*, in which the exocyclic phenyl group was replaced by a bulky *tert*-butyl group.^[20b] Indeed, the combination of both features, a rigid cyclic framework and the steric differentiation at the silicon atom, facilitated promising diastereoselectivity of 92:8 in the dehydrogenative Si–O coupling [*rac-6* → (^{Si}*S**,*S**)-**7a**, entry 4].^[5a] An even more refined survey on this basis clearly demonstrates the scope and limitations of this general structural motif (entries 5–7). With an isopropyl instead of a *tert*-butyl group (*rac-4a* → *rac-4b*^[16b]), diastereoselectivity decreased yet being by far higher than those for acyclic silanes [*rac-6* → (^{Si}*S**,*S**)-**7b**, entry 5].

A similar effect was observed with silaindane *rac-5a*^[23] equipped with a bulky *tert*-butyl group [*rac-6* → (^{Si}*S**,*S**)-**15a**, entry 6]. While diastereoselection was slightly diminished, a distinct acceleration of the reaction rate was monitored. The higher reactivity of the silane *rac-5a* in comparison to silatetralines *rac-4* is likely to be connected with the increased Lewis acidity of the silicon atom in a strained silacycle.^[24] Therefore, *rac-5a* constitutes an alternative for the resolution of alcohols otherwise unreactive in this catalysis. Recently, a kinetic resolution of tertiary propargylic alcohols with highly enantioenriched (^{Si}*R*)- or (^{Si}*S*)-**5a**^[23] was achieved following exactly this strategy.^[5b] It is, however, interesting to note that a further decrease of steric bulk results in a complete collapse of diastereoselectivity; isopropyl-bearing silaindane *rac-5b*^[16d] yielded silyl ether (^{Si}*S**,*S**)-**15b** in a diastereomeric ratio of 52:48 (entry 7). The high reactivity of *rac-5b* also made this silane highly susceptible to hydrolysis with traces of water present in the reaction mixture; addition of powdered molecular sieves effectively suppressed this side-reaction.

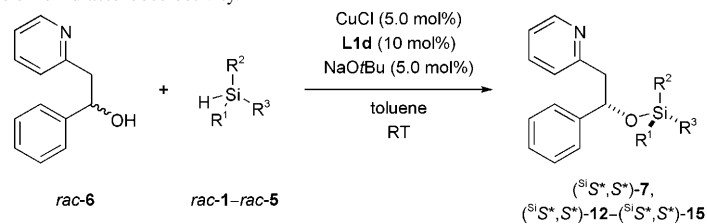
Kinetic resolution of 2-(pyridin-2-yl)ethanols with sterically hindered silatetraline: After having identified suitable conditions for diastereoselective dehydrogenative Si–O coupling, this novel kinetic resolution process was tested with a

selection of pyridyl ethanols. For this, highly enantiomerically enriched silane **4a** (93–99% *ee*) was used. This privileged silane (cf. Table 3) was made available in both enantiomeric forms by a classic resolution of its corresponding (–)-menthyl ethers (99% *ee*) or—at the early stages of this project—by reversed kinetic resolution with an enantiopure pyridyl alcohol (≤96% *ee*).^[20b,25]

Routinely, 0.60 equiv of enantioenriched silane (^{Si}*S*)-**4a** or (^{Si}*R*)-**4a**, respectively, were used along with a catalyst loading of 5.0 mol% at room temperature. After full consumption of the resolving agent, conversion of approximately 55% was determined by ¹H NMR spectroscopy; diastereomeric ratios were determined by ¹H NMR spectroscopic analysis of the crude reaction mixture as well.

This survey commenced with variation of the substituent at the stereogenic carbon. Tables 4 and 5 summarize the results for kinetic resolutions arranged by the silane enantiomer (^{Si}*S*)-**4a** (Table 4) and (^{Si}*R*)-**4a** (Table 5). Since the diastereomeric ratios for the obtained silyl ethers are biased by conversion when using enantioenriched silane (Tables 4 and 5, column 8), the diastereomeric ratios of silyl ethers for the reaction with racemic silane *rac-4a* are also listed (column 9) in order to compare the efficiency of kinetic resolution for different substrates. As expected, phenyl-substituted alcohol *rac-6* cleanly underwent the kinetic resolution when exposed to CuCl/**L1d**/NaOtBu and 0.60 equiv of silane (^{Si}*S*)-**4a** (94% *ee*) [*rac-6* → (^{Si}*R*,*R*)-**7a**, Table 4, entry 1]. At 58% conversion, a promising enantiomeric excess for the slow-reacting enantiomer (*S*)-**6** (88% *ee*) was detected as well as a reduced diastereomeric ratio for silyl ether (^{Si}*R*,*R*)-**7a** compared to the racemic series due to >50% conversion. Gratiifyingly, chemical yields of both silyl ether (^{Si}*R*,*R*)-**7a** and alcohol (*S*)-**6** were almost quantitative. Straightforward separation of alcohol and silyl ether by flash column chromatography underscores the preparative simplicity of this methodology. As supported by 2- as well as 1-naphthyl substituted alcohols *rac-16* and *rac-24*, respectively, aryl substitution at the stereogenic carbon is tolerated (Table 4, entry 2; Table 5, entry 1). At a conversion of 54%, the remaining alcohol (*S*)-**16** showed 75% *ee* [*rac-16* → (^{Si}*R*,*R*)-**20a**, Table 4, entry 2]. Kinetic resolution of related *rac-24* furnished silyl ether (^{Si}*S*,*S*)-**29a** in good diastereoselectivity (d.r. 92:8 in the racemic series) along with enantioenriched alcohol in (*R*)-**24** (80% *ee* at 57% conversion) [*rac-24* → (^{Si}*S*,*S*)-**29a**, Table 5, entry 1]. These findings were substantiated in the kinetic resolution of other substituents with sp²-hybridization at carbon, allylic alcohols *rac-17* and *rac-25* [Table 4, entry 3;

Table 3. Influence of silane substitution on diastereoselectivity.^[a]



Entry	Silane (equiv)	<i>t</i> [h]	Conv [%] ^[b]	Silyl ether	Yield [%] ^[c]	d.r. ^[d]
1	<i>rac</i> -1 (0.55)	3	51	 <i>(S^i,S^*)</i> -12	51 (47)	57:43
2	<i>rac</i> -2 (0.55)	12	52	 <i>(S^i,S^*)</i> -13	51 (34)	59:41
3	<i>rac</i> -3 (0.55)	4	52	 <i>(S^i,S^*)</i> -14	51 (45)	66:34
4	<i>rac</i> -4a (0.50)	20	47	 <i>(S^i,S^*)</i> -7a	44 (50)	92:8
5	<i>rac</i> -4b (1.20)	24	100	 <i>(S^i,S^*)</i> -7b	94	83:17
6	<i>rac</i> -5a (0.55)	1	52	 <i>(S^i,S^*)</i> -15a	49 (47)	86:14
7 ^[e]	<i>rac</i> -5b (1.20)	4	100	 <i>(S^i,S^*)</i> -15b	85	52:48

For footnotes [a]–[d], see Table 2. [e] Reaction performed in the presence of powdered molecular sieves 4 Å.

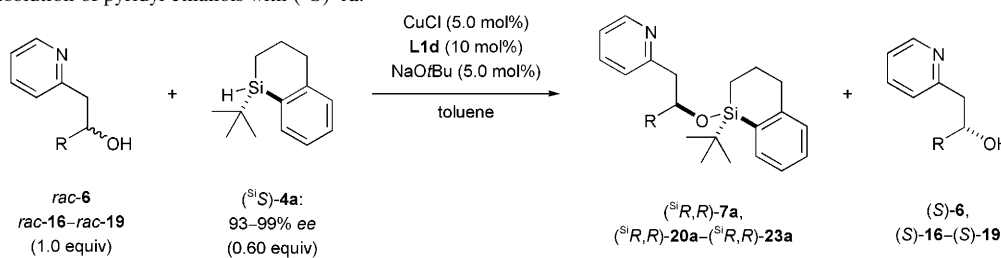
Table 5, entry 2]. In the former case, diminished diastereoselection in the racemic series (d.r. 88:12) was also manifested in the kinetic resolution with (^{Si}S)-**4a** (94% *ee*) delivering (*S*)-**17** in moderate enantiopurity (69% *ee*) [*rac*-**17**→(^{Si}R,*R*)-**21a**, Table 4, entry 3]. Similarly, cinnamyl alcohol *rac*-**25** underwent kinetic resolution with (^{Si}R)-**4a** to give (*R*)-**25** (74% *ee*) with essentially the same stereoselectivity [*rac*-**25**→(^{Si}S,*S*)-**30a**, Table 5, entry 2]. The propargylic alcohol *rac*-**26** was tested with an increased amount of silane (^{Si}R)-**4a** (0.65 equiv) [*rac*-**26**→(^{Si}S,*S*)-**31a**, Table 5, entry 3]. Higher conversion (63%) in turn led to the isolation of the remaining alcohol (*R*)-**26** in good enantioselectivity, although the diastereoselectivity was only moderate (d.r. 85:15 in the racemic series). Concomitant (*Z*)-selective alkyne reduction was observed, which might be explained by a directed hydrogenation in the presence of dihydrogen and a copper catalyst; this is in accordance with a report by Stryker and coworkers.^[26] For the (*Z*)-cinnamyl alcohol, an enantiomeric excess of 57% *ee* was detected; minor amounts of the (*Z*)-cinnamyl silyl ether showed a diastereomeric ratio of 90:10.

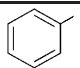
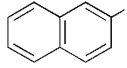
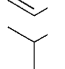

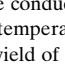
In contrast, pyridyl ethanols with branched alkyl substituents emerged as poor substrates (Table 4, entries 4 and 5; Table 5, entry 4). Isopropyl substitution in *rac*-**18** significant-

ly lowered reactivity when exposed to silane (^{Si}S)-**4a**: Silyl ether (^{Si}R,*R*)-**22a** was only formed at elevated temperatures with modest diastereoselectivity (d.r. 81:19 in the racemic series); thus the optical purity of the remaining alcohol (*S*)-**18** (47% *ee*) failed to meet a synthetically useful level (Table 4, entry 4). For comparison, *rac*-**27** equipped with a cyclohexyl group emerged as poor as well and required elevated reaction temperatures for turnover [*rac*-**27**→(^{Si}S,*S*)-**32a**, Table 5, entry 4]. A substantial loss in reactivity also complicated dehydrogenative Si–O coupling of sterically demanding *tert*-butyl group-containing alcohol *rac*-**19** (Table 4, entry 5). Low conversion of 46% was only amenable in the presence of 10 mol% of copper catalyst and 1.2 equiv of resolving agent (^{Si}S)-**4a**. As a consequence—irrespective of the promising diastereoselectivity of isolated silyl ether (^{Si}R,*R*)-**23a** (d.r. 94:6 as against 95:5 in the racemic series)—the enantiomeric purity of isolated alcohol (*S*)-**19** remained disappointing. Conversely, a simple methyl group as in *rac*-**28** was tolerated by stereogenic silane (^{Si}R)-**4a** although the optical purity of (*S*)-**28** at 58% conversion was only moderate [*rac*-**28**→(^{Si}S,*R*)-**33a**, Table 5, entry 5].

Since an enantioimpure reagent was used in almost all kinetic resolutions (see below), the assignment of selectivity factors according to Kagan is not straightforward.^[27] In

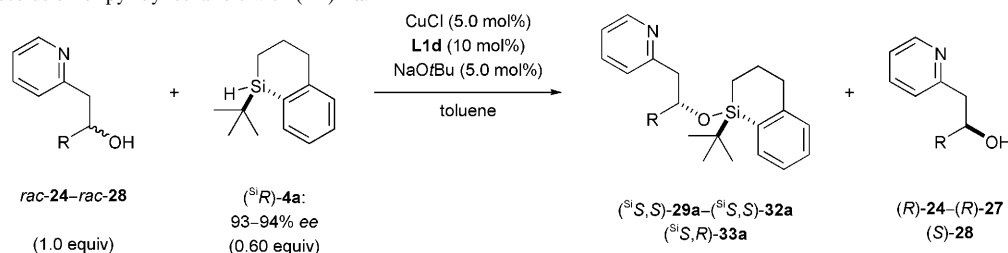
Table 4. Kinetic resolution of pyridyl ethanols with (^{Si}S)-**4a**.^[a]



Entry	Racemic alcohol	R	Silane		Silyl ether	Yield [%] ^[c]	d.r. ^[d,e]	d.r. ^[d,f]	Recovered alcohol		Conv [%] ^[h]	s ^[i]	s' ^[j]	
			<i>ee</i> [%] ^[b]	<i>T</i> [°C]					Yield [%] ^[c]	<i>ee</i> [%] ^[b,g]				
1	<i>rac</i> - 6		94	20	(^{Si} R, <i>R</i>)- 7a	57	84:16	92:8	(<i>S</i>)- 6	42	88 (–)	58	30	13
2	<i>rac</i> - 16		99	20	(^{Si} R, <i>R</i>)- 20a	50	85:15	91:9	(<i>S</i>)- 16	42	75 (–)	54	26	10
3	<i>rac</i> - 17		94	20	(^{Si} R, <i>R</i>)- 21a	48	88:12	88:12	(<i>S</i>)- 17	50	69 (–)	50	17	11
4	<i>rac</i> - 18		93	60	(^{Si} R, <i>R</i>)- 22a	47	80:20	81:19	(<i>S</i>)- 18	38	47 (+)	51	8.2	4.4
5 ^[k]	<i>rac</i> - 19		94	110	(^{Si} R, <i>R</i>)- 23a	40	94:6	95:5	(<i>S</i>)- 19	53	68 (+)	46	58	18

[a] All reactions were conducted using CuCl (5.0 mol%), ligand **L1d** (10 mol%), and NaOtBu (5.0 mol%) with a substrate concentration of 0.1 M in toluene at the indicated temperature. [b] Determined by HPLC analysis using Daicel Chiralcel or Chiralpak columns providing baseline separation of enantiomers. [c] Isolated yield of analytically pure material after flash chromatography; yield calculation is based on initial amount of racemic alcohol. [d] Determined by ¹H NMR spectroscopy of the crude reaction mixture by integration of baseline-separated resonance signals of the diastereomers. [e] Diastereomeric ratio in the enantioenriched series is biased by conversion (>50%). [f] Diastereomeric ratio in the racemic series (not biased by conversion). [g] Sense of optical rotation is given in parentheses. [h] Monitored by ¹H NMR spectroscopy and determined by integration of baseline-separated resonance signals. [i] Theoretical selectivity factor based on enantioimpure silane calculated from $s = \ln[(1-0.5)(1-de_{rac})] / \ln[(1-0.5)(1+de_{rac})]$; de_{rac} in the racemic series corresponds to *ee* of the recovered alcohol in the enantiomeric series at exactly 50% conversion (provided that both follow identical kinetics). [j] Apparent selectivity factor when using an enantioimpure reagent calculated from: $s' = \ln[(1-C)(1-ee)] / \ln[(1-C)(1+ee)]$ where $ee = ee/100$ and $C = \text{conversion}/100$.^[7b] [k] 1.2 equiv of (^{Si}S)-**4a** and a catalyst loading of 10 mol% used.

Table 5. Kinetic resolution of pyridyl ethanol with (^{Si}R)-4a.^[a]



Entry	Racemic alcohol	R	Silane		Silyl ether	Yield [%] ^[c]	d.r. ^[d,e]	d.r. ^[d,f]	Recovered alcohol	Yield [%] ^[c]	ee [%] ^[b,g]	Conv [%] ^[b]	s ^[j]	s' ^[j]
			ee [%] ^[b]	T [°C]										
1	<i>rac-24</i>		93	20	(^{Si,S,S})- 29a	57	84:16	92:8	(<i>R</i>)- 24	43	80 (+)	57	30	9.6
2	<i>rac-25</i>		93	20	(^{Si,S,S})- 30a	56	87:13	88:12	(<i>R</i>)- 25	43	74 (-)	57	17	7.6
3 ^[k,l]	<i>rac-26</i>		93	20	(^{Si,S,S})- 31a	51	74:26	85:15	(<i>R</i>)- 26	31	89 (-)	63	12	9.0
4 ^[k]	<i>rac-27</i>		94	60	(^{Si,S,S})- 32a	55	73:27	n.d.	(<i>R</i>)- 27	43	42 (+)	56	n.d.	2.9
5	<i>rac-28</i>		93	20	(^{Si,S,R})- 33a	57	76:24	n.d.	(<i>S</i>)- 28	42	73 (+)	58	n.d.	6.8

For footnotes[a]–[j], see Table 4. [k] 0.65 equiv of (^{Si}R)-4a used. [l] Reaction accompanied by partial Z-selective alkyne reduction: (^{Si,S,S})-**31a** contaminated with 7% of Z-alkene [Z/E 93:7, d.r. (Z Isomer) 90:10] and (*R*)-**26** contaminated with 21% of Z-alkene (57% ee). n.d. = not determined.

Tables 4 and 5, two different calculations are used to assign a selectivity factor: $s^{[7b]}$ and, additionally, the apparent selectivity factor s' .^[27] The former value s is calculated based on the diastereomeric ratio observed in the racemic series; the diastereomeric excess should correspond to the enantiomeric excess at exactly 50% conversion when an enantiopure silane is used and is thus not biased by conversion and the somewhat critical determination of the latter by ¹H NMR spectroscopy.^[28] However, this assumption requires that both reaction setups follow identical kinetics. The latter value s' considers the enantiopurity of the resolving chiral silane as being 100% and is calculated based on the enantiomeric purity of the recovered alcohol at a given conversion.^[7b] Thus, s' may be regarded as a minimal value. For suitable substrates containing aryl, alkenyl and alkynyl moieties at the stereogenic carbon, s ranges between 12 and 30; s' is in the range of 7.6 to 13. Alkyl substitution in turn leads to difficult-to-resolve substrates; this is not only reflected in $2.9 < s' < 6.8$ (except $s' = 18$ for *t*Bu) but also by the insufficient reactivity of these derivatives.

Variation of the pending donor: In order to explore the scope of the present concept, a survey of potential donors other than the 2-pyridyl unit was of particular interest. For this purpose, several heteroaromatic substituents with a Lewis basic site were screened to explore reactivity and stereoselectivity (Table 6). Initially, phenyl substitution at the stereogenic carbon was retained as a common motif for all

secondary alcohols *rac-34*–*rac-40*. The “pyridine-type motif” offered considerable generality (Table 6, entries 1–3): Secondary alcohol *rac-34* equipped with a 2-picolinyl group gave almost identical results as parent alcohol *rac-6* [*rac-34* → (^{Si,R,R})-**41a**, entry 1]; at 60% conversion, remaining alcohol (*S*)-**34** was isolated in useful enantiomeric purity (89% ee, $s = 30$, $s' = 11$). Not surprisingly, 2-quinolyl substitution was also tolerated; kinetic resolution of *rac-35* with (^{Si}S)-**4a** (99% ee) delivered enantioenriched (*S*)-**35** (82% ee at 57% conversion, $s = 26$, $s' = 10$) along with silyl ether (^{Si,R,R})-**42a** (d.r. 81:19 or 91:9 in the racemic series) (entry 2). In contrast, the isoquinoline derivative *rac-36* displayed significantly reduced stereoselectivity when subjected to (^{Si}S)-**4a** (97% ee): At 52% conversion, diastereoselectivity of silyl ether (^{Si,R,R})-**43a** (d.r. 83:17) and enantiomeric excess of the slow-reacting (*S*)-**36** (54% ee or $s' = 5.0$) was disappointing (entry 3). Subsequently, secondary alcohols *rac-37* and *rac-38* containing an oxazole subunit were subjected to the Si–O coupling (entries 4 and 5). To our delight, 4,5-dimethyloxazol-2-yl ring exhibited good donor capability for copper(I); the latter fact was apparent from the observed diastereoselectivity for *rac-37* in the racemic series (d.r. 89:11). When using enantiopure silane (^{Si}S)-**4a** (99% ee), moderate enantiomeric excess for recovered (*S*)-**37** (65% ee, $s = 19$, $s' = 6.2$) was detected [*rac-37* → (^{Si,R,R})-**44a**, entry 4]. As opposed to *rac-37*, benzoxazole derivative *rac-38* emerged as incompatible to the reaction conditions: The low solubility of alcohol *rac-38* in toluene required a solvent switch to benzene (or

Table 6. Variation of the donor (Do) in the kinetic resolution (^{Si}S)-**4a**.^[a]

Entry	Racemic alcohol	Donor	Silane		Silyl ether	Yield [%] ^[c]	d.r. ^[d,e]	d.r. ^[d,f]	Recovered alcohol		Conv [%] ^[h]	s ^[i]	s' ^[j]	
			ee [%] ^[b]	T [°C]					Yield [%] ^[c]	ee [%] ^[g]				
1	<i>rac</i> - 34		98	20	(^{Si} <i>R,R</i>)- 41a	57	77:23	92:8	(<i>S</i>)- 34	32	89 (-)	60	30	11
2	<i>rac</i> - 35		99	20	(^{Si} <i>R,R</i>)- 42a	52	81:19	91:9	(<i>S</i>)- 35	36	82 (-)	57	26	10
3	<i>rac</i> - 36		97	40	(^{Si} <i>R,R</i>)- 43a	46	83:17	n.d.	(<i>S</i>)- 36	47	54 (-)	52	n.d.	5.0
4	<i>rac</i> - 37		99	20	(^{Si} <i>R,R</i>)- 44a	50	79:21	89:11	(<i>S</i>)- 37	41	65 (-)	55	19	6.2
5 ^[k,l]	<i>rac</i> - 38		-	20	(^{Si} <i>R*,R*</i>)- 45a	8	-	83:17	<i>rac</i> - 38	0	-	18	9.1	-
6 ^[k,l]	<i>rac</i> - 39		-	20	(^{Si} <i>R*,R*</i>)- 46a	26	-	92:8	<i>rac</i> - 39	4	-	48	30	-
7	<i>rac</i> - 40		-	20	(^{Si} <i>R*,R*</i>)- 47a	24	-	65:35	<i>rac</i> - 40	70	-	27	2.4	-

For footnotes[a]–[j], see Table 4. [k] Low solubility of *rac*-**38** and *rac*-**39** in toluene; instead benzene was used as a solvent. [l] Reaction was accompanied by decomposition of alcohols *rac*-**38** and *rac*-**39** under the reaction conditions.

toluene/THF). Nevertheless, efficient kinetic resolution was thwarted by a competitive decomposition under the standard reaction conditions; retro-1,2-addition predominantly led to methyl benzoxazole along with benzaldehyde. For this reason, no alcohol *rac*-**38** was recovered in the reaction with *rac*-**4a**; poor conversion to silyl ether (^{Si}*R*,R**)-**45a** (d.r. 83:17) was achieved (entry 5). The same situation was seen for related benzothiazole derivative *rac*-**39**; despite good diastereoselection in the formation of silyl ether (^{Si}*R*,R**)-**46a** (d.r. 92:8), almost no alcohol was recovered from the reaction mixture (entry 6). A comparison with the thiophene derivative *rac*-**40** suggests that sulfur in *rac*-**39** is less likely to coordinate to copper(I); low conversion and diastereoselectivity corroborate this interpretation [*rac*-**40** → (^{Si}*R*,R**)-**47a**, entry 7].

Kinetic resolution with sterically hindered silatetraline: Privileged *tert*-butyl-substituted silatetraline **4a** was compatible with a reasonable substrate range. However, for sterically

crowded substrates its reactivity emerged as insufficient.^[5b] Based on an analysis of the assumed transition state, σ -bond metathesis **D** (cf. Scheme 1), we reasoned that increased Lewis acidity at the silicon atom might enhance its reactivity since Si–O interaction is believed to be operating prior to the metathesis step. Therefore, we anticipated that embedding silicon into a strained carbocycle (strain release Lewis acidity^[24]) ought to produce higher reactivity of silatetraline derivatives **5** towards less reactive substrates. The validity of this reasoning was recently demonstrated to facilitate the Cu–H-catalyzed kinetic resolution of tertiary propargylic alcohols.^[5b]

A brief survey of the synthetic value of virtually enantiopure silane (^{Si}*R*)-**5a**^[23] as a resolving agent for donor-functionalized secondary alcohols revealed that, compared to silatetraline (^{Si}*R*)-**4a**, reactivity was significantly increased (Table 7). Kinetic resolutions were generally completed within a few hours or even minutes compared to approximately one day for **4a**; lower reaction temperatures were

Table 7. Kinetic resolution with silane (^{Si}R)-**5a**.^[a]

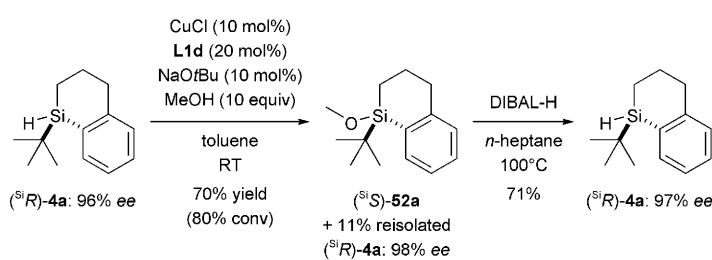
Entry	Racemic alcohol	R	Donor	Silyl ether	Yield [%] ^[c]		Recovered alcohol		Conv [%] ^[h]	s ^[i]	s ^[j]		
					d.r. ^[d,e]	d.r. ^[d,f]	Yield [%] ^[c]	ee [%] ^[b,g]					
1 ^[i,k]	<i>rac</i> - 6	Ph	2-pyridyl	(^{Si} S, _S)- 15a	51	77:23	86:14	(<i>R</i>)- 6	45	83 (+)	53	13	17
2	<i>rac</i> - 16	2-naphthyl	2-pyridyl	(^{Si} S, _S)- 48a	57	76:24	85:15	(<i>R</i>)- 16	38	69 (+)	58	12	5.9
3	<i>rac</i> - 24	1-naphthyl	2-pyridyl	(^{Si} S, _S)- 49a	55	77:23	88:12	(<i>R</i>)- 24	41	75 (+)	56	17	8.4
4	<i>rac</i> - 35	Ph	2-quinolyl	(^{Si} S, _S)- 50a	57	75:25	87:13	(<i>R</i>)- 35	40	74 (+)	58	15	7.1
5	<i>rac</i> - 37	Ph	4,5-dimethyl-oxazol-2-yl	(^{Si} S, _S)- 51a	55	74:26	86:14	(<i>R</i>)- 37	41	65 (+)	57	13	5.5

For footnotes[a]–[j], see Table 4. [j] 0.57 equiv of (^{Si}R)-**5a** used. [k] Reaction performed at 0 °C.

also possible using **5a** yet having only minor effect on stereoselectivity. Substrates *rac*-**6**, *rac*-**16** and *rac*-**24** with a 2-pyridyl donor and different aromatic R groups at the stereogenic carbon gave inferior results (Table 7, entries 1–3). At conversions of 53–58%, enantiomeric excesses of the remaining alcohols ranged from 69–83% ee; this is also reflected by the moderate diastereoselectivities for silyl ethers (^{Si}S,_S)-**15a**, (^{Si}S,_S)-**48a–49a** in the racemic series (85:15 ≤ d.r. ≤ 88:12). Isolated yields of both silyl ethers (^{Si}S,_S)-**15a**, (^{Si}S,_S)-**48a–49a** and alcohols (*R*)-**6**, (*R*)-**16** and (*R*)-**24** indicated again a good mass balance. Similar observations were made when two different donor functionalities were screened (entries 4 and 5). Kinetic resolution of quinolyl substituted *rac*-**35** and oxazole-bearing *rac*-**37** delivered enantioenriched alcohols (*R*)-**35** and (*R*)-**37** along with silyl ethers (^{Si}S,_S)-**50a** and (^{Si}S,_S)-**51a** in good yields and the expected stereoselectivities. Notably, the same enantiomers of the racemic alcohols were consumed by silatetraline (^{Si}R)-**4a** and silaindane (^{Si}R)-**5a** as secured by the sense of optical rotation.

Stereochemical course at the silicon atom: In order to rigorously exclude any racemization processes under the reaction conditions of the kinetic resolution, initial considerations had resulted in choosing a σ-bond metathesis reaction pathway instead of an approach based on chlorosilanes.^[15b] Although we anticipated an enantiospecific Si–O bond formation by Cu–H-catalyzed dehydrogenative coupling, experimental proof had not been accomplished yet. A simple two-step sequence consisting of methanolysis and subsequent reductive cleavage of a highly enantiomerically enriched silane (^{Si}R)-**4a** clarified this issue [(^{Si}R)-**4a** → (^{Si}S)-**52a** → (^{Si}R)-**4a**, Scheme 2].

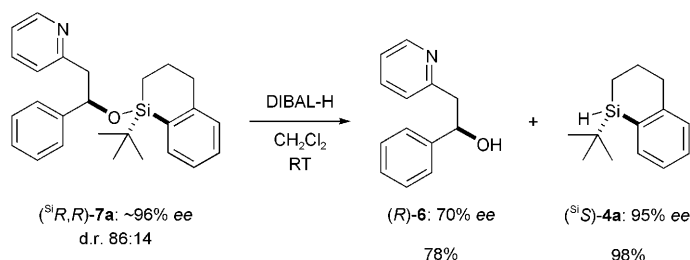
Since methanol is, of course, not donor-functionalized, the Cu–H-catalyzed methanolysis proceeded only sluggishly at higher catalyst loadings in the presence of excess of methanol [(^{Si}R)-**4a** → (^{Si}S)-**52a**]. Methyl ether (^{Si}S)-**52a** was contaminated with minor amounts of phosphine **L1d**. Along with (^{Si}S)-**52a**, starting silane (^{Si}R)-**4a** was isolated without de-



Scheme 2. Enantiospecific Si–O coupling and reductive Si–O cleavage.

tectable erosion of enantiomeric purity. The reductive cleavage using DIBAL–H at elevated temperature then liberated silane (^{Si}R)-**4a**;^[17,29] a comparison of HPLC analytical data confirmed retention of configuration for the overall sequence. This outcome is also in agreement with the expected double retention pathway for the two-step procedure.

At the beginning, the absolute configuration of the slow-reacting alcohols and newly formed silyl ethers were assigned by comparing the sign of optical rotation of recovered (*S*)-**6** with literature data^[30] (cf. Table 4, entry 1).^[5a] Relative and absolute configuration of silyl ether (^{Si}R,_R)-**7a** was further validated by stereospecific reductive cleavage of silyl ether (^{Si}R,_R)-**7a** that delivered (*R*)-**6** and (^{Si}S)-**4a** (Scheme 3). The latter reaction also demonstrates the feasibility of recovering the resolving silane in preserved enantiomeric purity.



Scheme 3. Recycling of the resolving reagent by stereospecific reductive Si–O cleavage.

Thus, absolute and relative configurations of both silyl ethers and alcohols are predictable provided that the absolute configuration of the resolving silane is known. Based on model substrate *rac*-**6**, configurational assignments for all other substrates were made. Crystalline material suitable for X-ray diffraction was obtained as well; the major diastereomer of silyl ether (^{Si}*R**,*R**)-**43a** (Figure 2) that was prepared from isoquinolyl-substituted alcohol *rac*-**36** and *rac*-**4a** and subsequent diastereoenrichment by flash chromatography confirmed the predicted relative configuration.

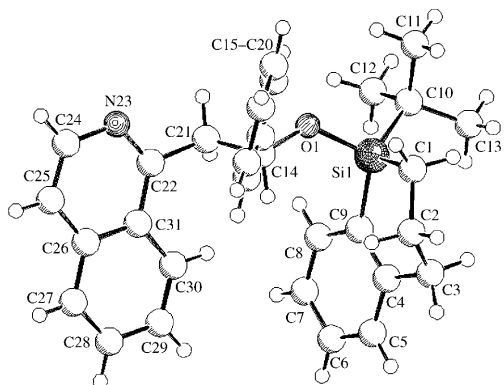
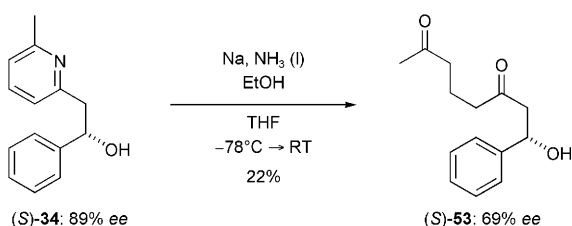


Figure 2. Molecular structure of (^{Si}*R**,*R**)-**43a**.

Reductive degradation of the pyridine donor: There is only a handful of methods available for the enzymatic^[30,31] and chemical^[32] kinetic resolution of pyridine-containing alcohols. As our procedure provides an enantioselective access to several, potentially synthetically useful motifs, we briefly looked into their subsequent chemistry. Danishefsky and co-workers had used 2,6-lutidines as 1,5-dicarbonyl equivalents in total synthesis.^[33] In our case, Birch reduction followed by acidic hydrolysis transformed (*S*)-**34** (89% *ee*) into diketone (*S*)-**53** (69% *ee*) in moderate chemical yield (Scheme 4), which compares well with the reported systems.^[33] Unfortunately, partial racemization thwarted any further applications.



Scheme 4. Danishefsky pyridine route: Access to enantioenriched 1,5-dicarbonyl compounds.

Mutual kinetic resolution: The present methodology holds interesting mechanistic peculiarities, which are closely linked to the reagent-controlled nature of this kinetic resolution strategy—a line of research that has been addressed to a

much smaller extent than prevailing catalyst-controlled processes. In the former scenario, the chiral resolving reagent should be literally enantiopure. At the beginning of this project, we were unable to prepare sufficient quantities of enantiopure silanes; enantiomeric excesses typically ranged from 93 to 96%.^[5a,20b] Yet, this issue is a superable problem since Kagan's precise predictions for reagent-controlled kinetic resolutions also give satisfying results when an enantiopure reagent is used and (pseudo-)first order kinetics are prevalent.^[27] Consequently, a mutual kinetic resolution^[7b] should be operative. Thus, not only the enantiomeric excess of the remaining alcohol but also of the resolving silane is expected to increase with conversion. To test for this, a kinetic resolution of standard substrate *rac*-**6** with silane (^{Si}*R*)-**4a** of low enantiopurity (32% *ee*) was monitored by ¹H NMR spectroscopy; aliquots of the reaction mixture were individually separated into silane, silyl ether and remaining alcohol by flash chromatography and subsequently analyzed by HPLC using a chiral stationary phase. Not only that the enantiomeric purity of the alcohol (*R*)-**6** gradually increased with time until reaching 35% *ee* at 52% conversion, the enantiomeric excess of unreacted silane (^{Si}*R*)-**4a** also rose to 48% *ee* at 51% conversion (Figure 3). These experimental observations are in accordance with Kagan's prediction for a (pseudo-)first order kinetic resolution.^[27]

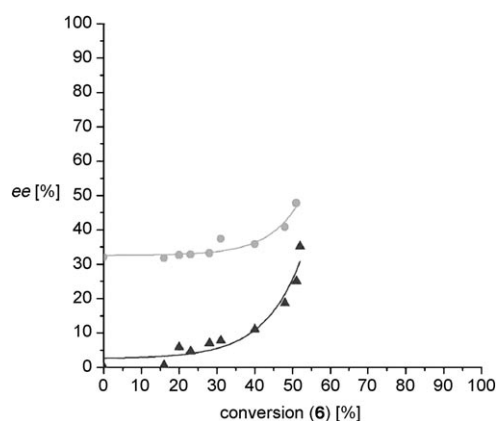


Figure 3. Mutual kinetic resolution using a scalemic silane: ▲: (*R*)-**6**, ●: (^{Si}*R*)-**4a**.

Quantum-chemical calculations: Density functional theory (DFT) and improved Moller–Plesset perturbation (SCS-MP2) calculations were performed with TURBOMOLE^[34] on the model reaction between (H₃P)₂CuOR (R = Me and *t*Bu) and Me₃SiH. We used the PBE^[35] functional for geometry optimizations and obtained single point energies with the hybrid functional B3LYP^[36] and the wavefunction method SCS-MP2.^[37] For all calculations, a triple zeta AO basis with additional polarization functions on the heavy atoms (TZVPP) was used.^[38]

With R = Me, we have identified a reaction path (Figure 4) for the Cu–H-catalyzed Si–O coupling via an transition structure (TS), in which the alkoxide is transferred to silicon yielding a four-center-intermediate (INT).

Although the intermediate has been characterized as a minimum by vibrational analysis, no according transition structure for its fragmentation towards the product complex was found. Note that in the course of the reaction (fragmentation of INT), the Me_3Si moiety must be rotated to achieve the tetrahedral geometry of the product. Relative energies for intermediates and TS are given in Table 8.

Table 8. Relative energies [kcal mol^{-1}] of stationary points for reaction in Figure 4.

Method ^[a]	Reactants	r-Complex	TS	Intermediate	p-Complex	Products
DFT-PBE	4.8	0.0	4.0	3.2	-11.7	-7.3
DFT-B3LYP	1.5	0.0	5.6	5.3	-13.7	-12.1
SCS-MP2	6.2	0.0	2.3	0.2	-15.7	-8.4

[a] TZVPP AO basis, DFT-PBE optimized geometries.

Although the reaction barrier and energies differ by some kcal mol^{-1} with the three methods, the qualitative description of the energy profile is the same: The energetic distinction between INT and TS is only very small. It is therefore not advisable to consider the reaction a “two-step”-process. With the SCS-MP2 method, the intermediate is almost isoenergetic to the r-complex and the barrier lower than 3 kcal mol^{-1} . In summary, the prereactive r-complex and the product p-complex stabilize reactants and products, the dehydrogenative Si–O coupling proceeds through an intermediate/transition structure with a very low barrier. It is exothermic and irreversible since the back reaction (Si–O reductive cleavage) requires a substantially larger activation energy than the Si–O coupling.

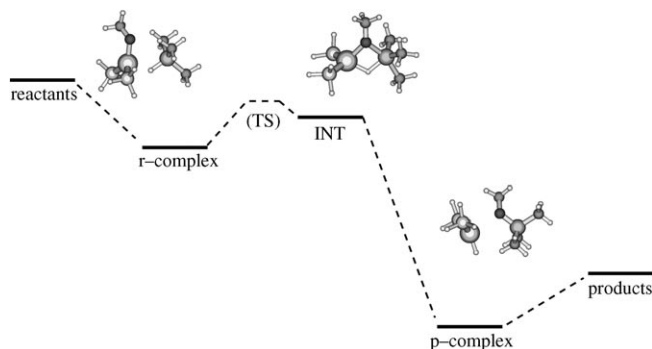


Figure 4. Energy profile (DFT-PBE/TZVPP) for the reaction of $(\text{H}_3\text{P})_2\text{CuOMe}$ and Me_3SiH .

The front-side attack at the silicon atom confirms the experimental observation that the substitution occurs under retention at the silicon atom. Although the four-center-intermediate (Figure 5) is energetically close to the reactant complex, the bond lengths and bond orders indicate an almost synchronous bond transfer that has proceeded about half the way towards the product. The compact nature of the intermediate is also reflected in the rather short Cu–Si distance (2.81 \AA). It is therefore reasonable to expect a high degree of stereochemical discrimination when the reaction

occurs between a chiral Si–H compound and a chiral copper(I) alkoxide.

To get an estimate of steric effects in the reaction, we have re-calculated the reaction with a *tert*-butoxy substituent. The larger substituent has a pronounced impact on the energy profile, as can be seen in Table 9. With $\text{OR} = \text{O}t\text{Bu}$, we were not able to locate a four-center-intermediate as with $\text{OR} = \text{OMe}$. Instead, optimization yielded the reactive or product complexes. These have higher relative energies compared to the isolated reactants or products than the corresponding methoxy complexes.

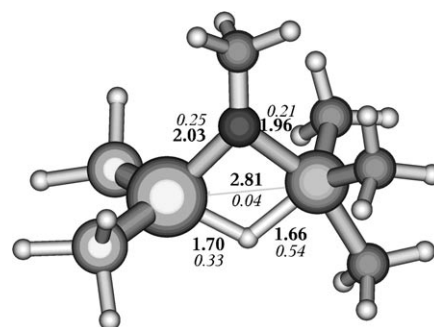


Figure 5. Optimized distances in \AA (DFT-PBE/TZVPP, bold) and Mulliken overlap populations (DFT-PBE/TZVP, italic) for the intermediate (INT) of the methoxide reaction. For comparison, optimized single bond lengths of the reactants and products at this level are Cu–O: 1.85 \AA , Cu–H: 1.54 \AA , Si–H: 1.51 \AA , and Si–O: 1.68 \AA .

The barrier of the reaction was estimated by calculating reaction paths of the Si–O bond formation and taking the highest point [$r(\text{Si–O}) = 1.89 \text{ \AA}$] as an approximation for the TS. Most notable are the decreased exothermicity and larger reaction barrier for $(\text{H}_3\text{P})_2\text{CuO}t\text{Bu}$. Although the calculated reaction is only a model using very small metal ligands, the barrier has more than doubled with all methods employed. The “best” method (SCS-MP2) predicts a 2.5-fold higher energy of the transition structure than in the reaction of the smaller copper(I) alkoxide. The retardation observed in the experiment using $\text{CuCl}/\text{NaO}t\text{Bu}$ with **L1d** is therefore nicely reproduced in this calculation.

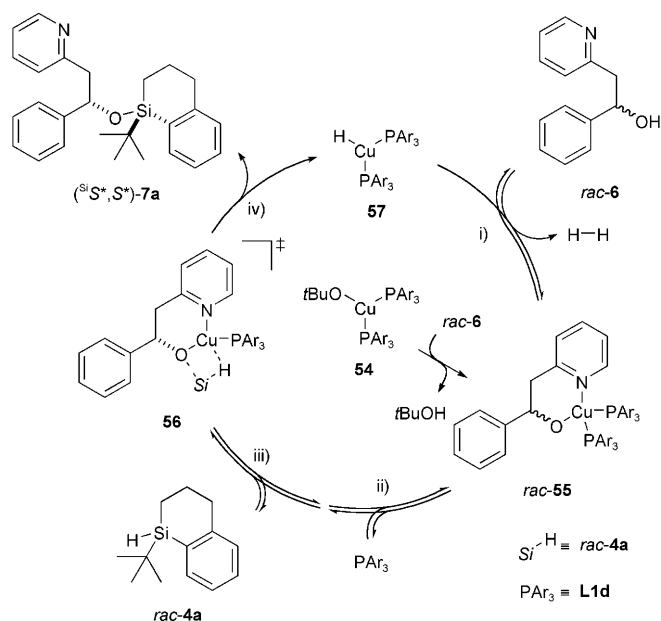
Proposed mechanism: Based on literature precedent,^[12–14,39] our stereochemical analysis, and the quantum-chemical calculations, we postulate a complete catalytic cycle. It comprises a four-step propagation as it is depicted in Scheme 5.

The catalysis is initiated by phosphine-stabilized copper(I) alkoxide^[11c,40] *rac*-**55** that is generated from **54** by alkoxide exchange. A single catalytic turnover generates copper(I) hydride **57**, which is the catalytically active species.^[12–14,39] In step i) dihydrogen is liberated from alcohol *rac*-**6** and copper(I) hydride **57** upon which copper(I) chelate *rac*-**55** is formed. Reversible and, likely, rate-limiting dissociation of a

Table 9. Relative energies [kcal mol⁻¹] of stationary points for reaction in Figure 4 with (H₃P)₂CuOtBu as copper(I) reagent.

Method ^[a]	Reactants	r-Complex	TS ^[b]	p-Complex	Products
DFT-PBE	3.6	0.0	9.4	-7.4	-4.1
DFT-B3LYP	0.1	0.0	12.6	-9.9	-9.1
SCS-MP2	5.4	0.0	5.9	-10.8	-4.4

[a] TZVPP AO basis, DFT-PBE optimized geometries. [b] Highest point of the reaction coordinate for Si–O bond formation [$r(\text{Si}-\text{O})=1.89 \text{ \AA}$].



Scheme 5. Proposed catalytic cycle.

phosphine ligand in step ii) generates a 16-electron intermediate that is prone to coordinative saturation by weakly coordinating silane **4a** in step iii). Step ii) could moreover facilitate a pseudo-first order scenario that is essential for good stereoselectivity in the kinetic resolution. At this stage, diastereodiscrimination between enantiomeric copper(I) alkoxide complexes must occur. Hence, one out of the two enantiomers of **6** is preferentially funneled out of the reaction mixture via rapid, exergonic σ -bond metathesis, transient intermediate or transition state **56** in step iv).^[12–14,39] By this, the major diastereomer (^SS*,S*)-**7a** is formed along with the regeneration of copper(I) hydride **57**. Importantly, the diastereodiscriminating event is step iv) and thus all preceding steps must be in equilibrium. A relative to the irreversible step rapid exchange of both enantiomers of pyridyl alcohol **6** at copper(I) chelate **55** is essential for this.

Conclusion

In summary, we presented a full account of our investigations towards a unique kinetic resolution strategy. The important parameters governing reactivity and diastereoselectivity of this reagent-controlled process are 1) moderately

electron-rich monophosphines generate sufficiently reactive copper(I) complexes, 2) two-point binding of the substrate to the transition metal, that is formation of a six-membered chelate by coordination of both the alkoxy group and an sp²-hybridized nitrogen donor, is essential, and 3) the use of sterically hindered, silicon-stereogenic silanes with silatetralines being less reactive but more selective than the corresponding silaindanes. With ideal catalyst–substrate–silane combinations a selectivity factor of $s=30$ are possible.

The Si–O coupling step itself is a particularly interesting feature of this Cu–H catalysis. It proceeds with stereoretention at the silicon atom passing through an assumed four-centered transition state. Quantum-chemical calculations do indeed support a σ -bond metathesis, yet its precise nature—transition state or, more likely, transient intermediate—remains slightly uncertain.

Experimental Section

General information: Reagents for starting material syntheses, CuCl as well as ligands **L1a**, **L1g** and **L2** were purchased from commercial sources. NaOtBu was freshly prepared and stored under argon atmosphere. Silanes **rac-1**,^[18] **rac-2**,^[19] **rac-3**,^[20a] **4a**,^[20b] **rac-4b**,^[16b] **rac-5b**,^[16d] ligands **L1b–L1f**,^[41] as well as **L3a** and **L3b**,^[42] were prepared according to known procedures. All reactions were performed in flame-dried glassware under a static pressure of argon. Liquids and solutions were transferred with syringes or double-ended needles. Toluene (Na/benzophenone) and CH₂Cl₂ (CaH₂) were dried by continuous distillation from the indicated drying reagent prior to use. Analytical thin-layer chromatography (TLC) was performed on silica gel SIL G-25 glass plates by Macherey-Nagel (Germany); for flash column chromatography, silica gel 60 (40–63 μm , 230–400 mesh, ASTM) by Merck (Germany), cyclohexane and *tert*-butyl methyl ether as solvent were used. ¹H and ¹³C NMR spectra were recorded in CDCl₃ on Bruker AM 400, AV 400, DRX 500, Varian INOVA 500 and Unity plus 600 spectrometers. HPLC analyses were performed with an Agilent 1200 or a Merck-Hitachi LaChrom 7100 instrument using chiral stationary phases (Daicel Chiralcel OD-H, AD-H, OJ-R, OJ-RH or Chiralpak IB columns). Mass spectra were recorded with Finnigan MAT TSO 7000 (EI, CI) or Bruker MicroTOF (ESI) instruments. IR spectra were recorded on Perkin–Elmer Paragon 1000 or Varian 3100 FT-IR instruments. Optical rotations were measured in a 1 dm cuvette on a Perkin–Elmer 341 polarimeter. Elemental analyses were conducted on a Vario EL instrument from Elementaranalysensysteme GmbH. Experimental details for the synthesis and resolution of silane **5a**, as well as for the preparation of racemic secondary alcohols and characterization data for all silyl ethers are included in the Supporting Information of this article.

(^SR)-1-*tert*-Butyl-1-silaindane [(^SR)-5a**]:**^[23] $R_f=0.77$ (cyclohexane); $[\alpha]_D^{20}=+42.4$ ($c=1.01$, CHCl₃), $[\alpha]_{578}^{20}=+44.1$, $[\alpha]_{546}^{20}=+49.0$, $[\alpha]_{436}^{20}=+72.9$, $[\alpha]_{365}^{20}=+85.4$; HPLC (Daicel Chiralcel OJ-R, 20 °C, MeOH/H₂O 80:20, flow rate 0.50 mL min⁻¹, $\lambda=230$ nm): $t_R=24.3$ min [(^SR)-**5a**], 27.8 min [(^SS)-**5a**]; ¹H NMR (400 MHz, CDCl₃): $\delta=1.02$ (s, 9H), 1.04 (dddd, $J=15.2, 7.9, 6.0, 3.0$ Hz, 1H), 1.16 (dddd, $J=15.2, 8.8, 7.1, 3.2$ Hz, 1H), 3.08–3.14 (m, 2H), 4.45 (dd, $J=J=3.1$ Hz, 1H), 7.20 (m, 1H), 7.24–7.28 (m, 1H), 7.32 (m, 1H), 7.61 ppm (m, 1H); ¹³C NMR (100 MHz, CDCl₃): $\delta=5.3, 17.1, 26.8, 32.5, 125.7, 125.8, 129.7, 133.4, 135.2, 154.5$ ppm; IR (film): $\tilde{\nu}=3056$ (s), 2923 (s), 2108 (s), 1589 (s), 1463 (s),

1441 cm⁻¹ (s); HRMS (EI): *m/z*: calcd for C₁₂H₁₈Si [M⁺]: 190.1178, found: 190.1173; elemental analysis calcd (%) for C₁₂H₁₈Si (190.4): C 75.71, H 9.53; found: C 75.72, H 9.52.

General procedure for Cu–H-catalyzed kinetic resolution of donor-functionalized alcohols (GP 1): A flame-dried Schlenk tube equipped with a magnetic stirring bar was charged with a mixture of CuCl (0.050 equiv) and **L1d** (0.10 equiv) under argon atmosphere. The solids were suspended in degassed, anhydrous toluene. After the addition of NaOrBu (0.050 equiv), a pale yellow solution formed within 1–2 min stirring at room temperature. Subsequently, a solution of racemic alcohol (1.0 equiv) in toluene (0.2 M) and silane (0.60 equiv) in toluene (0.24 M) were sequentially added via syringe. The resulting bright yellow solution (0.1 M relating to the alcohol) occasionally showed gas evolution and was maintained at the indicated temperature until complete consumption of silane as monitored by ¹H NMR spectroscopic analysis. After addition of *tert*-butyl methyl ether (8 mL) and a small portion of silica gel, the solvents were evaporated. Purification by flash column chromatography on silica gel using cyclohexane/*tert*-butyl methyl ether mixtures afforded the analytically pure silyl ether along with the unreacted alcohol as oils or solids.

(S)-1-Phenyl-2-(pyridin-2-yl)ethanol [(S)-6] (Table 4, entry 1): According to GP 1, starting from *rac*-**6** (79.7 mg, 0.400 mmol, 1.00 equiv), (^SS)-**4a** (49.1 mg, 0.240 mmol, 0.600 equiv, 94% *ee*), CuCl (2.0 mg, 0.020 mmol, 0.050 equiv), **L1d** (13.9 mg, 0.0400 mmol, 0.100 equiv) and NaOrBu (1.9 mg, 0.020 mmol, 0.050 equiv) in toluene (4.0 mL), silyl ether (^S*R,R*)-**7a** (92 mg, 57%, d.r. 84:16) and alcohol (S)-**6** (33 mg, 42%, 88% *ee*) were isolated as analytically pure materials. (S)-**6**: M.p. 107°C (CH₂Cl₂/*tert*-butyl methyl ether); *R*_f=0.12 (cyclohexane/*tert*-butyl methyl ether 1:1); [α]_D²⁰=−31.4 (*c*=1.05, CHCl₃), [α]_D²⁰₅₇₈=−32.7, [α]_D²⁰₅₄₆=−35.9, [α]_D²⁰₄₃₆=−48.9, [α]_D²⁰₃₆₅=−37.0; HPLC (Daicel Chiralcel OD-H, 20°C, *n*-heptane/*i*PrOH 90:10, flow rate 0.80 mL min⁻¹, λ=230 nm): *t*_R=12.4 min [(R)-**6**], 18.1 min [(S)-**6**]; ¹H NMR (400 MHz, CDCl₃): δ=3.08–3.20 (m, 2H), 5.18 (dd, *J*=8.3, 3.9 Hz, 1H), 5.69 (brs, 1H), 7.11 (brd, *J*=8.0 Hz, 1H), 7.18 (ddd, *J*=7.6, 4.9, 1.1 Hz, 1H), 7.24–7.29 (m, 1H), 7.32–7.37 (m, 2H), 7.41–7.45 (m, 2H), 7.61 (ddd, *J*=7.6, 1.0 Hz, 1H), 8.54 ppm (ddd, *J*=4.9, 1.6, 1.0 Hz, 1H); ¹³C NMR (100 MHz, CDCl₃): δ=45.8, 73.4, 121.8, 123.9, 125.9, 127.3, 128.4, 136.9, 144.2, 148.7, 158.9 ppm; IR (cuvette/CDCl₃): $\tilde{\nu}$ =3308 (s), 3089 (s), 3066 (s), 3031 (s), 2906 (m), 1952 (w), 1882 (w), 1760 (w), 1597 (s), 1570 (s), 1495 (m), 1475 (s), 1453 (s), 1438 (s), 1338 (m), 1279 (m), 1280 (m), 1150 (m), 1100 (m), 1078 (w), 1054 (m), 1028 (m), 1019 (m), 1001 (w), 903 (m), 816 (w), 735 cm⁻¹ (w); LRMS (CI/NH₃): *m/z*: 200 [M+H⁺]; elemental analysis calcd (%) for C₁₃H₁₃NO (199.3): C 78.36, H 6.58, N 7.03; found: C 78.13, H 6.63, N 6.95.

(S)-1-(Naphth-2-yl)-2-(pyridin-2-yl)ethanol [(S)-16] (Table 4, entry 2): According to GP 1, starting from *rac*-**16** (99.7 mg, 0.400 mmol, 1.00 equiv), (^SS)-**4a** (49.1 mg, 0.240 mmol, 0.600 equiv, 99% *ee*), CuCl (2.0 mg, 0.020 mmol, 0.050 equiv), **L1d** (13.9 mg, 0.0400 mmol, 0.100 equiv) and NaOrBu (1.9 mg, 0.020 mmol, 0.050 equiv) in toluene (4.0 mL), silyl ether (^S*R,R*)-**20a** (90 mg, 50%, d.r. 85:15) and alcohol (S)-**16** (42 mg, 42%, 75% *ee*) were isolated as analytically pure materials. (S)-**16**: M.p. 99–100°C (cyclohexane/*tert*-butyl methyl ether); *R*_f=0.28 (cyclohexane/*tert*-butyl methyl ether 1:2); [α]_D²⁰=−21.2 (*c*=1.01, CHCl₃), [α]_D²⁰₅₇₈=−23.0, [α]_D²⁰₅₄₆=−25.4, [α]_D²⁰₄₃₆=−34.0, [α]_D²⁰₃₆₅=−27.7; HPLC (Daicel Chiralcel AD-H, 20°C, *n*-heptane/*i*PrOH 80:20, flow rate 1.00 mL min⁻¹, λ=230 nm): *t*_R=14.0 min [(R)-**16**], 16.6 min [(S)-**16**]; ¹H NMR (400 MHz, CDCl₃): δ=3.21 (dd, *J*=15.2, 4.7 Hz, 1H), 3.23 (dd, *J*=15.2, 7.5 Hz, 1H), 5.35 (dd, *J*=7.4, 4.7 Hz, 1H), 5.88 (brs, 1H), 7.11 (ddd, *J*=7.8, 2.1, 1.0 Hz, 1H), 7.19 (ddd, *J*=7.6, 4.9, 1.2 Hz, 1H), 7.46 (m, 2H), 7.55 (dd, *J*=8.6, 1.6 Hz, 1H), 7.61 (ddd, *J*=7.7, 1.9 Hz, 1H), 7.81–7.85 (m, 3H), 7.89–7.91 (m, 1H), 8.56 ppm (ddd, *J*=4.9, 1.8, 0.9 Hz, 1H); ¹³C NMR (100 MHz, CDCl₃): δ=45.7, 73.5, 121.8, 123.9, 124.3, 124.5, 125.7, 126.0, 127.7, 128.1, 132.9, 133.5, 137.0, 141.6, 148.7, 159.8 ppm; IR (cuvette/CDCl₃): $\tilde{\nu}$ =3305 (m), 3060 (w), 1595 (s), 1475 (s), 1437 (s), 1058 cm⁻¹ (s); HRMS (EI): *m/z*: calcd for C₁₇H₁₅NO [M⁺]: 249.1154, found: 249.1160; elemental analysis calcd (%) for C₁₇H₁₅NO (249.3): C 81.90, H 6.06, N 5.62; found: C 81.64, H 6.10, N 5.55.

(S)-1-(Pyridin-2-yl)but-3-en-2-ol [(S)-17] (Table 4, entry 3): According to GP 1, starting from *rac*-**17** (59.7 mg, 0.400 mmol, 1.00 equiv), (^SS)-**4a**

(49.1 mg, 0.240 mmol, 0.600 equiv, 94% *ee*), CuCl (2.0 mg, 0.020 mmol, 0.050 equiv), **L1d** (13.9 mg, 0.0400 mmol, 0.100 equiv) and NaOrBu (1.9 mg, 0.020 mmol, 0.050 equiv) in toluene (4.0 mL), silyl ether (^S*R,R*)-**21a** (67 mg, 48%, d.r. 88:12) and alcohol (S)-**17** (30 mg, 50%, 69% *ee*) were isolated as analytically pure materials. (S)-**17**: M.p. 46°C (CH₂Cl₂); *R*_f=0.41 (CH₂Cl₂/methanol 95:5); [α]_D²⁰=−1.15 (*c*=0.420, CHCl₃), [α]_D²⁰₅₇₈=−0.77, [α]_D²⁰₅₄₆=+0.38, [α]_D²⁰₄₃₆=+10.0, [α]_D²⁰₃₆₅=+44.2; HPLC (Daicel Chiralcel OD-H, 20°C, *n*-heptane/*i*PrOH 98:2, flow rate 0.80 mL min⁻¹, λ=230 nm): *t*_R=21.8 min [(S)-**17**], 24.2 min [(R)-**17**]; ¹H NMR (500 MHz, CDCl₃): δ=2.93 (dd, *J*=14.8, 8.6 Hz, 1H), 3.02 (dd, *J*=14.8, 3.2 Hz, 1H), 4.59 (dddd, *J*=8.5, 5.7, 3.2, *J*=1.6 Hz, 1H), 5.11 (ddd, *J*=10.4, *J*=1.6 Hz, 1H), 5.23 (brs, 1H), 5.31 (ddd, *J*=17.0, *J*=1.6 Hz, 1H), 5.94 (ddd, *J*=17.0, 10.4, 5.7 Hz, 1H), 7.13–7.18 (m, 2H), 7.62 (ddd, *J*=7.6, 1.9 Hz, 1H), 8.50 ppm (brd, *J*=4.4 Hz, 1H); ¹³C NMR (125 MHz, CDCl₃): δ=43.3, 72.0, 114.7, 121.7, 123.9, 136.9, 140.3, 148.7, 159.8 ppm; IR (cuvette/CDCl₃): $\tilde{\nu}$ =3317 (s), 3088 (s), 3018 (s), 2079 (s), 2915 (m), 1849 (w), 1645 (w), 1597 (s), 1571 (s), 1476 (s), 1438 (s), 1366 (w), 1327 (w), 1284 (w), 1236 (w), 1198 (m), 1150 (m), 1111 (m), 1099 (m), 1078 (s), 1051 (s), 1032 (s), 992 (s), 963 (s), 843 (s), 808 cm⁻¹ (s); LRMS (CI/NH₃): *m/z*: 150 [M+H⁺]; elemental analysis calcd (%) for C₉H₁₁NO (149.2): C 72.26, H 7.43, N 9.39; found: C 72.24, H 7.50, N 9.20.

(S)-3-Methyl-1-(pyridin-2-yl)butan-2-ol [(S)-18] (Table 4, entry 4): According to GP 1, starting from *rac*-**18** (66.1 mg, 0.400 mmol, 1.00 equiv), (^SS)-**4a** (49.1 mg, 0.240 mmol, 0.600 equiv, 93% *ee*), CuCl (2.0 mg, 0.020 mmol, 0.050 equiv), **L1d** (13.9 mg, 0.0400 mmol, 0.100 equiv) and NaOrBu (1.9 mg, 0.020 mmol, 0.050 equiv) in toluene (4.0 mL), silyl ether (^S*R,R*)-**22a** (69 mg, 47%, d.r. 80:20) and alcohol (S)-**18** (25 mg, 38%, 47% *ee*) were isolated as colorless oils. (S)-**18**: *R*_f=0.11 (cyclohexane/*tert*-butyl methyl ether 1:1); [α]_D²⁰=+5.32 (*c*=0.470, CHCl₃), [α]_D²⁰₅₇₈=+5.96, [α]_D²⁰₅₄₆=+7.87, [α]_D²⁰₄₃₆=+25.5, [α]_D²⁰₃₆₅=+78.5; HPLC (Daicel Chiralcel OD-H, 20°C, *n*-heptane/*i*PrOH 98:2, flow rate 0.80 mL min⁻¹, λ=230 nm): *t*_R=12.7 min [(R)-**18**], 14.4 min [(S)-**18**]; ¹H NMR (400 MHz, CDCl₃): δ=0.98 (d, *J*=6.7 Hz, 3H), 1.01 (d, *J*=6.8 Hz, 3H), 1.74 (qqd, *J*=6.7, 5.9 Hz, 1H), 2.83 (dd, *J*=14.8, 9.5 Hz, 1H), 2.90 (dd, *J*=14.8, 2.4 Hz, 1H), 3.77 (ddd, *J*=9.4, 5.7, 2.6 Hz, 1H), 5.03 (brs, 1H), 7.12–7.17 (m, 2H), 7.61 (ddd, *J*=7.7, 1.9 Hz, 1H), 8.48 ppm (ddd, *J*=4.8, 1.8, 0.8 Hz, 1H); ¹³C NMR (100 MHz, CDCl₃): δ=18.1, 18.7, 33.6, 40.3, 76.0, 121.5, 123.8, 136.8, 148.6, 160.9 ppm; IR (cuvette/CDCl₃): $\tilde{\nu}$ =3337 (s), 3142 (w), 3089 (w), 3076 (w), 3018 (w), 2963 (s), 2933 (s), 2910 (s), 2896 (s), 2874 (s), 1596 (s), 1570 (s), 1475 (s), 1438 (s), 1384 (m), 1367 (m), 1340 (w), 1311 (w), 1279 (m), 1238 (w), 1198 (m), 1170 (w), 1150 (m), 1130 (w), 1097 (m), 1079 (m), 1051 (s), 1039 (s), 1007 (s), 997 (s), 921 (s), 887 (m), 845 (m), 795 cm⁻¹ (m); LRMS (CI/NH₃): *m/z*: 166 [M+H⁺]; elemental analysis calcd (%) for C₁₀H₁₅NO (165.2): C 72.69, H 9.15, N 8.48; found: C 72.47, H 9.22, N 8.34.

(S)-3,3-Dimethyl-1-(pyridin-2-yl)butan-2-ol [(S)-19] (Table 4, entry 5): According to GP 1, starting from *rac*-**19** (71.7 mg, 0.400 mmol, 1.00 equiv), (^SS)-**4a** (98.1 mg, 0.480 mmol, 1.20 equiv, 94% *ee*), CuCl (4.0 mg, 0.040 mmol, 0.10 equiv), **L1d** (27.7 mg, 0.0800 mmol, 0.200 equiv) and NaOrBu (3.8 mg, 0.040 mmol, 0.10 equiv) in toluene (4.0 mL), silyl ether (^S*R,R*)-**22a** (61 mg, 40%, d.r. 94:6) and alcohol (S)-**19** (38 mg, 53%, 68% *ee*) were isolated as colorless oils. (S)-**19**: *R*_f=0.59 (cyclohexane/*tert*-butyl methyl ether 1:2); [α]_D²⁰=+18.1 (*c*=0.36, CHCl₃), [α]_D²⁰₅₇₈=+18.6, [α]_D²⁰₅₄₆=+23.3, [α]_D²⁰₄₃₆=+61.1, [α]_D²⁰₃₆₅=+164; HPLC (Daicel Chiralcel AD-H, 20°C, *n*-heptane/*i*PrOH 98:2, flow rate 0.80 mL min⁻¹, λ=230 nm): *t*_R=15.2 min [(R)-**19**], 29.9 min [(S)-**19**]; ¹H NMR (400 MHz, CDCl₃): δ=1.00 (s, 9H), 2.76 (dd, *J*=14.7, 10.5 Hz, 1H), 2.92 (dd, *J*=14.7, 1.9 Hz, 1H), 3.66 (dd, *J*=10.5, 1.9 Hz, 1H), 5.03 (brs, 1H), 7.14 (dd, *J*=7.6, 5.0 Hz, 1H), 7.16 (brd, *J*=7.9 Hz, 1H), 7.62 (ddd, *J*=7.6, 1.9 Hz, 1H), 8.48 ppm (ddd, *J*=4.8, 1.6, 0.9 Hz, 1H); ¹³C NMR (100 MHz, CDCl₃): δ=25.9, 34.8, 38.7, 78.7, 121.5, 123.8, 136.9, 148.6, 161.2 ppm; IR (cuvette/CDCl₃): $\tilde{\nu}$ =3325 (s), 3142 (w), 3090 (w), 3076 (w), 3063 (w), 3017 (w), 2961 (s), 2910 (s), 2870 (s), 1595 (s), 1570 (m), 1478 (s), 1437 (s), 1389 (w), 1364 (s), 1328 (w), 1312 (w), 1279 (w), 1243 (m), 1213 (w), 1201 (w), 1177 (w), 1150 (w), 1101 (m), 1071 (s), 1049 (m), 1013 (s), 966 (m), 837 (s), 806 cm⁻¹ (s); HRMS (ESI): *m/z*: calcd for C₁₁H₁₈NO [M+H⁺]: 180.1383, found: 180.1396; elemental analysis calcd (%) for C₁₁H₁₇NO (179.3): C 73.70, H 9.56, N 7.81; found: C 73.42, H 9.74, N 7.67.

(R)-1-(Naphth-1-yl)-2-(pyridin-2-yl)ethanol [(R)-24] (Table 5, entry 1): According to GP 1, starting from *rac*-**16** (99.7 mg, 0.400 mmol, 1.00 equiv), (*S*)-**4a** (49.1 mg, 0.240 mmol, 0.600 equiv, 93% *ee*), CuCl (2.0 mg, 0.020 mmol, 0.050 equiv), **L1d** (13.9 mg, 0.0400 mmol, 0.100 equiv) and NaOrBu (1.9 mg, 0.020 mmol, 0.050 equiv) in toluene (4.0 mL), silyl ether (*S,S*)-**29a** (102 mg, 57%, d.r. 84:16) and alcohol (*R*)-**24** (43 mg, 43%, 80% *ee*) were isolated as analytically pure materials. (*R*)-**24**: M.p. 114°C (cyclohexane/*tert*-butyl methyl ether); $R_f=0.17$ (cyclohexane/*tert*-butyl methyl ether 1:1); $[\alpha]_D^{20}=+171$ ($c=0.320$, CHCl₃), $[\alpha]_{578}^{20}=+178$, $[\alpha]_{546}^{20}=+203$, $[\alpha]_{436}^{20}=+345$, $[\alpha]_{365}^{20}=+504$; HPLC (Daicel Chiralcel OD-H, 20°C, *n*-heptane/*i*PrOH 90:10, flow rate 0.80 mL min⁻¹, $\lambda=230$ nm): $t_R=18.6$ min [(*S*)-**24**], 24.0 min [(*R*)-**24**]; ¹H NMR (400 MHz, CDCl₃): $\delta=3.25$ (dd, $J=15.3$, 9.7 Hz, 1H), 3.35 (dd, $J=15.4$, 2.7 Hz, 1H), 5.85 (brs, 1H), 5.98 (dd, $J=9.0$, 2.7 Hz, 1H), 7.11 (brd, $J=7.8$ Hz, 1H), 7.22 (ddd, $J=7.6$, 5.0, 1.1 Hz, 1H), 7.47–7.54 (m, 3H), 7.63 (ddd, $J=7.6$, 1.9 Hz, 1H), 7.77–7.81 (m, 2H), 7.88–7.91 (m, 1H), 8.12–8.16 (m, 1H), 8.60 ppm (ddd, $J=5.0$, 2.0, 1.0 Hz, 1H); ¹³C NMR (100 MHz, CDCl₃): $\delta=44.9$, 70.1, 121.9, 123.0, 123.3, 123.8, 125.4, 125.7, 126.0, 127.8, 129.0, 130.3, 133.8, 137.0, 139.5, 148.8, 160.0 ppm; IR (cuvette/CDCl₃): $\tilde{\nu}=3314$ (s), 3062 (s), 2906 (w), 1599 (s), 1570 (s), 1512 (m), 1475 (s), 1438 (s), 1394 (m), 1359 (w), 1325 (w), 1281 (w), 1189 (s), 1102 (m), 1067 (w), 1003 (w), 891 (s), 883 (s), 805 cm⁻¹ (s); LRMS (EI): m/z : 249 [M^+]; elemental analysis calcd (%) for C₁₇H₁₅NO (249.3): C 81.90, H 6.06, N 5.62; found: C 81.63, H 6.12, N 5.50.

(R,E)-4-Phenyl-1-(pyridin-2-yl)but-3-en-2-ol [(R)-25] (Table 5, entry 2): According to GP 1, starting from *rac*-**25** (90.1 mg, 0.400 mmol, 1.00 equiv), (*S*)-**4a** (49.1 mg, 0.240 mmol, 0.600 equiv, 93% *ee*), CuCl (2.0 mg, 0.020 mmol, 0.050 equiv), **L1d** (13.9 mg, 0.0400 mmol, 0.100 equiv) and NaOrBu (1.9 mg, 0.020 mmol, 0.050 equiv) in toluene (4.0 mL), silyl ether (*S,S*)-**30a** (99 mg, 56%, d.r. 87:13) and alcohol (*R*)-**25** (38 mg, 43%, 74% *ee*) were isolated as analytically pure materials. (*R*)-**25**: $R_f=0.24$ (cyclohexane/*tert*-butyl methyl ether 1:2); $[\alpha]_D^{20}=-67.5$ ($c=0.440$, CHCl₃), $[\alpha]_{578}^{20}=-71.4$, $[\alpha]_{546}^{20}=-82.5$, $[\alpha]_{436}^{20}=-163$, $[\alpha]_{365}^{20}=-326$; HPLC (Daicel Chiralcel OD-H, 20°C, *n*-heptane/*i*PrOH 90:10, flow rate 0.80 mL min⁻¹, $\lambda=230$ nm): $t_R=17.9$ min [(*R*)-**25**], 20.5 min [(*S*)-**25**]; ¹H NMR (500 MHz, CDCl₃): $\delta=3.03$ (dd, $J=15.5$, 8.5 Hz, 1H), 3.10 (dd, $J=15.2$, 3.5 Hz, 1H), 4.78 (dddd, $J=8.5$, 6.0, 3.5, 1.3 Hz, 1H), 5.48 (brs, 1H), 6.31 (dd, $J=15.7$, 5.8 Hz, 1H), 6.68 (dd, $J=15.7$, 1.6 Hz, 1H), 7.16–7.20 (m, 2H), 7.20–7.24 (m, 1H), 7.28–7.32 (m, 2H), 7.36–7.39 (m, 2H), 7.64 (ddd, $J=7.6$, 1.9 Hz, 1H), 8.52 ppm (ddd, $J=4.7$, 1.9, 1.0 Hz, 1H); ¹³C NMR (125 MHz, CDCl₃): $\delta=43.6$, 71.8, 121.8, 123.9, 126.6, 127.5, 128.6, 130.0, 131.7, 136.9, 137.1, 148.7, 159.7 ppm; IR (cuvette/CDCl₃): $\tilde{\nu}=3306$ (s), 3143 (w), 3084 (m), 3063 (m), 3028 (s), 2908 (m), 1596 (s), 1570 (s), 1494 (s), 1475 (s), 1438 (s), 1326 (w), 1307 (w), 1188 (m), 1150 (m), 1101 (m), 1088 (m), 1069 (s), 1050 (s), 1029 (s), 1001 (s), 968 (s), 921 (s), 904 (m), 892 (m), 888 (m), 809 cm⁻¹ (s); LRMS (EI): m/z : 225 [M^+]; elemental analysis calcd (%) for C₁₅H₁₅NO (225.3): C 79.97, H 6.71, N 6.22; found: C 79.82, H 6.66, N 6.24.

(R)-4-Phenyl-1-(pyridin-2-yl)but-3-in-2-ol [(R)-26] (Table 5, entry 3): According to GP 1, starting from *rac*-**26** (89.3 mg, 0.400 mmol, 1.00 equiv), (*S*)-**4a** (53.1 mg, 0.260 mmol, 0.650 equiv, 93% *ee*), CuCl (2.0 mg, 0.020 mmol, 0.050 equiv), **L1d** (13.9 mg, 0.0400 mmol, 0.100 equiv) and NaOrBu (1.9 mg, 0.020 mmol, 0.050 equiv) in toluene (4.0 mL), silyl ether (*S,S*)-**31a** (87 mg, 51%, d.r. 74:26) and alcohol (*R*)-**26** (38 mg, 31%, 89% *ee*) were isolated as yellowish oils. Silyl ether (*S,S*)-**31a** was contaminated with 7% the silyl ether of *Z*-alkene [*Z/E* 93:7, d.r. (*Z* isomer) 90:10]; (*R*)-**26** contained 21% of (*Z*)-alkene (57% *ee*) as determined by ¹H NMR spectroscopy. (*R*)-**26**: $R_f=0.29$ (cyclohexane/*tert*-butyl methyl ether 1:2); $[\alpha]_D^{20}=-3.94$ ($c=0.330$, CHCl₃), $[\alpha]_{578}^{20}=-5.15$, $[\alpha]_{546}^{20}=-6.67$, $[\alpha]_{436}^{20}=-20.6$; HPLC (Daicel Chiralcel OD-H, 20°C, *n*-heptane/*i*PrOH 90:10, flow rate 0.80 mL min⁻¹, $\lambda=230$ nm): $t_R=15.9$ min [(*R*)-**26**], 24.4 min [(*S*)-**26**]; ¹H NMR (500 MHz, CDCl₃): $\delta=3.24$ (dd, $J=15.1$, 7.2 Hz, 1H), 3.30 (dd, $J=15.1$, 3.8 Hz, 1H), 5.08 (dd, $J=7.2$, 3.8 Hz, 1H), 5.57 (brs, 1H), 7.16–7.29 (m, 5H), 7.29–7.37 (m, 2H), 7.67 (ddd, $J=7.8$, 1.9 Hz, 1H), 8.52 ppm (brd, $J=4.7$ Hz, 1H); ¹³C NMR (125 MHz, CDCl₃): $\delta=43.6$, 62.3, 84.6, 89.7, 122.0, 122.9, 123.9, 128.3, 128.3, 131.8, 137.0, 148.7, 159.0 ppm; IR (cuvette/CDCl₃): $\tilde{\nu}=3305$ (s), 3084 (m), 3063 (m), 3020 (s), 2977 (s), 2930 (m), 1597 (s), 1571 (s), 1491 (s), 1476 (s), 1438 (s), 1389 (w), 1367 (w), 1325 (w), 1283 (w), 1235 (w), 1200 (m), 1151

(w), 1100 (s), 1053 (s), 1032 (s), 1001 (s), 936 (m), 926 (s), 919 (s), 841 (s), 795 cm⁻¹ (s); HRMS (EI): m/z : calcd for C₁₅H₁₃NO [M^+]: 223.0993, found: 223.0997. (*Z*)-alkene: HPLC (Daicel Chiralcel OD-H, 20°C, *n*-heptane/*i*PrOH 90:10, flow rate 0.80 mL min⁻¹, $\lambda=230$ nm): $t_R=10.9$ min (*S* enantiomer of *Z*-alkene), 13.9 min (*R* enantiomer of *Z*-alkene); ¹H NMR (500 MHz, CDCl₃): $\delta=3.02$ (dd, $J=14.9$, 3.5 Hz, 1H), 3.07 (dd, $J=15.1$, 8.2 Hz, 1H), 5.01 (dddd, $J=8.5$, 3.2, 1.2 Hz, 1H), 5.57 (brs, 1H), 5.77 (dd, $J=11.3$, 9.1 Hz, 1H), 6.57 (brd, $J=11.3$ Hz, 1H), 7.13 (brd, $J=7.9$ Hz, 1H), 7.16–7.29 (m, 2H), 7.29–7.37 (m, 4H), 7.62 (ddd, $J=7.6$, 1.9 Hz, 1H), 8.50 ppm (brd, $J=5.0$ Hz, 1H); ¹³C NMR (125 MHz, CDCl₃): $\delta=43.3$, 67.4, 121.8, 124.1, 127.2, 128.2, 128.3, 129.0, 131.1, 133.5, 136.8, 148.7, 159.9 ppm; HRMS (EI): m/z : calcd for C₁₅H₁₃NO [M^+]: 225.1154, found: 225.1150.

(R)-1-Cyclohexyl-2-(pyridin-2-yl)ethanol [(R)-27] (Table 5, entry 4): According to GP 1, starting from *rac*-**27** (82.1 mg, 0.400 mmol, 1.00 equiv), (*S*)-**4a** (53.1 mg, 0.260 mmol, 0.650 equiv, 93% *ee*), CuCl (2.0 mg, 0.020 mmol, 0.050 equiv), **L1d** (13.9 mg, 0.0400 mmol, 0.100 equiv) and NaOrBu (1.9 mg, 0.020 mmol, 0.050 equiv) in toluene (4.0 mL), silyl ether (*S,S*)-**32a** (90 mg, 55%, d.r. 73:27) and alcohol (*R*)-**27** (35 mg, 43%, 42% *ee*) were isolated as analytically pure materials. (*R*)-**27**: M.p. 35°C (cyclohexane/*tert*-butyl methyl ether); $R_f=0.26$ (cyclohexane/*tert*-butyl methyl ether 1:1); $[\alpha]_D^{20}=-5.82$ ($c=0.550$, CHCl₃), $[\alpha]_{578}^{20}=-6.36$, $[\alpha]_{546}^{20}=-7.64$, $[\alpha]_{436}^{20}=-18.5$, $[\alpha]_{365}^{20}=-50.4$; HPLC (Daicel Chiralcel OD-H, 20°C, *n*-heptane/*i*PrOH 98:2, flow rate 0.80 mL min⁻¹, $\lambda=230$ nm): $t_R=7.8$ min [(*R*)-**27**], 8.7 min [(*S*)-**27**]; ¹H NMR (400 MHz, CDCl₃): $\delta=1.05$ –1.31 (m, 5H), 1.38–1.47 (m, 1H), 1.63–1.70 (m, 1H), 1.72–1.82 (m, 3H), 1.94 (m, 1H), 2.85 (dd, $J=14.9$, 9.2 Hz, 1H), 2.92 (dd, $J=14.9$, 2.6 Hz, 1H), 3.77 (ddd, $J=9.2$, 5.9, 2.6 Hz, 1H), 5.04 (brs, 1H), 7.11–7.16 (m, 2H), 7.61 (ddd, $J=7.7$, 1.9 Hz, 1H), 8.47 ppm (dd, $J=5.6$, 1.9 Hz, 1H); ¹³C NMR (100 MHz, CDCl₃): $\delta=26.3$, 26.4, 26.7, 28.6, 29.1, 40.5, 43.6, 75.3, 121.5, 123.8, 136.8, 148.6, 160.9 ppm; IR (cuvette/CDCl₃): $\tilde{\nu}=3333$ (s), 3142 (w), 3089 (w), 3076 (w), 3018 (w), 2929 (s), 2854 (s), 1597 (s), 1570 (m), 1475 (s), 1450 (s), 1437 (s), 1345 (w), 1312 (w), 1277 (m), 1262 (m), 1228 (m), 1193 (m), 1175 (m), 1150 (m), 1131 (m), 1102 (m), 1051 (m), 1034 (s), 1002 (m), 990 (m), 907 (m), 841 (m), 809 cm⁻¹ (m); LRMS (CI/NH₃): m/z : 206 [$M+H^+$]; elemental analysis calcd (%) for C₁₅H₁₉NO (205.3): C 76.06, H 9.33, N 6.82; found: C 75.95, H 9.50, N 6.64.

(S)-1-(Pyridin-2-yl)propan-2-ol [(S)-28] (Table 5, entry 5): According to GP 1, starting from *rac*-**28** (54.9 mg, 0.400 mmol, 1.00 equiv), (*S*)-**4a** (49.1 mg, 0.240 mmol, 0.600 equiv, 93% *ee*), CuCl (2.0 mg, 0.020 mmol, 0.050 equiv), **L1d** (13.9 mg, 0.0400 mmol, 0.100 equiv) and NaOrBu (1.9 mg, 0.020 mmol, 0.050 equiv) in toluene (4.0 mL), silyl ether (*S,S*)-**33a** (77 mg, 57%, d.r. 76:24) and alcohol (*R*)-**27** (23 mg, 42%, 73% *ee*) were isolated as analytically pure materials. (*S*)-**28**: $R_f=0.25$ (CH₂Cl₂/MeOH 97:3); $[\alpha]_D^{20}=+5.71$ ($c=0.350$, CHCl₃), $[\alpha]_{578}^{20}=+6.29$, $[\alpha]_{546}^{20}=+5.15$, $[\alpha]_{436}^{20}=-3.43$, $[\alpha]_{365}^{20}=-43.7$; HPLC (Daicel Chiralcel AD-H, 20°C, *n*-heptane/*i*PrOH 98:2, flow rate 0.80 mL min⁻¹, $\lambda=230$ nm): $t_R=34.9$ min [(*S*)-**28**], 43.3 min [(*R*)-**28**]; ¹H NMR (500 MHz, CDCl₃): $\delta=1.26$ (d, $J=6.3$ Hz, 3H), 2.84 (dd, $J=15.0$, 8.4 Hz, 1H), 2.89 (dd, $J=15.0$, 3.3 Hz, 1H), 4.23 (dq, $J=8.4$, 6.3, 3.3 Hz, 1H), 5.08 (brs, 1H), 7.12–7.17 (m, 2H), 7.62 (ddd, $J=7.7$, 1.9 Hz, 1H), 8.49 ppm (ddd, $J=4.9$, 1.8, 0.9 Hz, 1H); ¹³C NMR (125 MHz, CDCl₃): $\delta=32.1$, 45.0, 67.2, 121.6, 123.7, 136.8, 148.7, 160.3 ppm; IR (cuvette/CDCl₃): $\tilde{\nu}=3343$ (s), 3142 (w), 3087 (w), 3018 (w), 2974 (s), 2932 (m), 2903 (m), 1596 (s), 1570 (s), 1476 (s), 1438 (s), 1374 (w), 1331 (w), 1283 (w), 1198 (m), 1150 (m), 1128 (m), 1100 (w), 1078 (m), 1052 (s), 1027 (m), 1001 (m), 937 (s), 930 (s), 840 (s), 795 cm⁻¹ (s); HRMS (ESI): m/z : calcd for C₈H₁₁NONa [$M+Na^+$]: 160.0733, found: 160.0729.

(S)-1-Phenyl-2-(6-methylpyridin-2-yl)ethanol [(S)-34] (Table 6, entry 1): According to GP 1, starting from *rac*-**34** (85.3 mg, 0.400 mmol, 1.00 equiv), (*S,S*)-**4a** (49.1 mg, 0.240 mmol, 0.600 equiv, 98% *ee*), CuCl (2.0 mg, 0.020 mmol, 0.050 equiv), **L1d** (13.9 mg, 0.0400 mmol, 0.100 equiv) and NaOrBu (1.9 mg, 0.020 mmol, 0.050 equiv) in toluene (4.0 mL), silyl ether (*S,S*)-**41a** (94 mg, 57%, d.r. 77:23) and alcohol (*S*)-**34** (27 mg, 32%, 89% *ee*) were isolated as analytically pure materials. (*S*)-**34**: M.p. 37°C (*tert*-butyl methyl ether); $R_f=0.26$ (cyclohexane/*tert*-butyl methyl ether 1:1); $[\alpha]_D^{20}=-30.9$ ($c=0.555$, CHCl₃), $[\alpha]_{578}^{20}=-32.2$,

$[\alpha]_{546}^{20} = -35.3$, $[\alpha]_{436}^{20} = -44.3$; HPLC (Daicel Chiralpak IB, 20°C, *n*-heptane/*i*PrOH 85:15, flow rate 0.80 mL min⁻¹, $\lambda = 230$ nm): $t_R = 7.6$ min [(*R*)-**34**], 8.9 min [(*S*)-**34**]; ¹H NMR (400 MHz, CDCl₃): $\delta = 2.54$ (s, 3H), 3.04 (dd, $J = 15.0$, 4.1 Hz, 1H), 3.09 (dd, $J = 15.0$, 8.0 Hz, 1H), 5.12 (dd, $J = 8.0$, 4.1 Hz, 1H), 6.32 (brs, 1H), 6.89 (d, $J = 7.7$ Hz, 1H), 7.02 (d, $J = 7.7$ Hz, 1H), 7.24 (dd, $J = J = 7.3$ Hz, 1H), 7.33 (dd, $J = J = 7.3$ Hz, 2H), 7.42 (d, $J = J = 7.3$ Hz, 2H), 7.48 ppm (dd, $J = J = 7.7$ Hz, 1H); ¹³C NMR (100 MHz, CDCl₃): $\delta = 24.2$, 45.3, 73.2, 120.6, 121.2, 125.7, 127.1, 128.2, 137.1, 144.1, 157.2, 159.0 ppm; IR (film): $\tilde{\nu} = 3317$ (s), 3062 (w), 2923 (w), 1596 (s), 1578 (m), 1457 (s), 1054 cm⁻¹ (s); LRMS (ESI): m/z : 236 [*M*+Na⁺]; elemental analysis calcd (%) for C₁₄H₁₅NO (213.3): C 78.84, H 7.09, N 6.57; found: C 78.88, H 6.96, N 6.41.

(*S*)-1-Phenyl-2-(quinolin-2-yl)ethanol [(*S*)-35**]** (Table 6, entry 2): According to GP 1, starting from *rac*-**35** (99.7 mg, 0.400 mmol, 1.00 equiv), (^{*S*}**S**)-**4a** (50.8 mg, 0.250 mmol, 0.625 equiv, 99% *ee*), CuCl (2.0 mg, 0.020 mmol, 0.050 equiv), **L1d** (13.9 mg, 0.0400 mmol, 0.100 equiv) and NaOtBu (1.9 mg, 0.020 mmol, 0.050 equiv) in toluene (4.0 mL), silyl ether (^{*S*}*R,R*)-**42a** (95 mg, 52%, d.r. 81:19) and alcohol (*S*)-**35** (36 mg, 36%, 82% *ee*) were isolated as analytically pure materials. (*S*)-**35**: M.p. 115–117°C (cyclohexane/*tert*-butyl methyl ether); $R_f = 0.46$ (cyclohexane/*tert*-butyl methyl ether 1:1); $[\alpha]_D^{20} = -59.0$ ($c = 0.990$, CHCl₃), $[\alpha]_{578}^{20} = -61.5$, $[\alpha]_{546}^{20} = -69.4$, $[\alpha]_{436}^{20} = -109$; HPLC (Daicel Chiralcel OD-H, 20°C, *n*-heptane/*i*PrOH 90:10, flow rate 0.80 mL min⁻¹, $\lambda = 230$ nm): $t_R = 15.9$ min [(*R*)-**35**], 20.5 min [(*S*)-**35**]; ¹H NMR (400 MHz, CDCl₃): $\delta = 3.31$ (dd, $J = 15.6$, 4.1 Hz, 1H), 3.34 (dd, $J = 15.6$, 8.1 Hz, 1H), 5.34 (dd, $J = 8.1$, 4.1 Hz, 1H), 6.17 (brs, 1H), 7.23 (d, $J = 8.4$ Hz, 1H), 7.26–7.31 (m, 1H), 7.34–7.40 (m, 2H), 7.47–7.51 (m, 2H), 7.54 (ddd, $J = 8.1$, 6.9, 1.2 Hz, 1H), 7.73 (ddd, $J = 8.5$, 6.9, 1.5 Hz, 1H), 7.81 (dd, $J = 8.1$, 1.4 Hz, 1H), 8.06–8.11 ppm (m, 2H); ¹³C NMR (100 MHz, CDCl₃): $\delta = 46.2$, 73.0, 122.2, 126.0, 126.3, 126.9, 127.4, 127.7, 128.4, 128.8, 129.9, 136.9, 144.1, 147.1, 160.6 ppm; IR (cuvette/CDCl₃): $\tilde{\nu} = 3308$ (m), 1600 (s), 1505 (s), 1426 (s), 1057 cm⁻¹ (s); LRMS (CI/NH₃): m/z : 250 [*M*+H⁺]; elemental analysis calcd (%) for C₁₇H₁₅NO (249.3): C 81.90, H 6.06, N 5.62; found: C 81.67, H 6.26, N 5.70.

(*S*)-2-(Isoquinolin-1-yl)-1-phenylethanol [(*S*)-36**]** (Table 6, entry 3): According to GP 1, starting from *rac*-**36** (99.7 mg, 0.400 mmol, 1.00 equiv), (^{*S*}**S**)-**4a** (45.0 mg, 0.220 mmol, 0.550 equiv, 97% *ee*), CuCl (2.0 mg, 0.020 mmol, 0.050 equiv), **L1d** (13.9 mg, 0.0400 mmol, 0.100 equiv) and NaOtBu (1.9 mg, 0.020 mmol, 0.050 equiv) in toluene (4.0 mL), silyl ether (^{*S*}*R,R*)-**43a** (83 mg, 46%, d.r. 83:17) and alcohol (*S*)-**36** (47 mg, 47%, 54% *ee*) were isolated as analytically pure materials. (*S*)-**36**: M.p. 115°C (*tert*-butyl methyl ether/CH₂Cl₂); $R_f = 0.31$ (cyclohexane/*tert*-butyl methyl ether 1:1); $[\alpha]_D^{20} = -45.9$ ($c = 0.810$, CHCl₃), $[\alpha]_{578}^{20} = -48.0$, $[\alpha]_{546}^{20} = -53.8$, $[\alpha]_{436}^{20} = -86.9$; HPLC (Daicel Chiralpak IB, 20°C, *n*-heptane/*i*PrOH 90:10, flow rate 0.80 mL min⁻¹, $\lambda = 230$ nm): $t_R = 15.9$ min [(*R*)-**36**], 19.1 min [(*S*)-**36**]; ¹H NMR (600 MHz, CDCl₃): $\delta = 3.57$ (dd, $J = 16.4$, 9.6 Hz, 1H), 3.72 (dd, $J = 16.4$, 2.2 Hz, 1H), 5.45 (dd, $J = 9.9$, 2.2 Hz, 1H), 6.19 (brs, 1H), 7.30–7.34 (m, 1H), 7.38–7.44 (m, 2H), 7.54–7.57 (m, 2H), 7.58 (ddd, $J = 8.2$, 6.9, 1.2 Hz, 1H), 7.60 (d, $J = 6.0$ Hz, 1H), 7.70 (ddd, $J = 8.2$, 6.8, 1.0 Hz, 1H), 7.84 (brd, $J = 8.2$ Hz, 1H), 8.05 (dd, $J = 8.4$, 0.8 Hz, 1H), 8.45 ppm (d, $J = 5.8$ Hz, 1H); ¹³C NMR (150 MHz, CDCl₃): $\delta = 41.9$, 72.4, 120.0, 124.8, 126.1, 127.3, 127.4, 127.5, 127.6, 128.5, 130.5, 136.2, 140.6, 144.1, 160.0 ppm; IR (cuvette/CDCl₃): $\tilde{\nu} = 3300$ (s), 3028 (s), 2923 (m), 2864 (s), 1603 (w), 1496 (s), 1454 (s), 1410 (m), 1317 (m), 1274 (m), 1209 (w), 1151 (w), 1072 (s), 1040 (s), 1027 (s), 953 (m), 917 (m), 831 (w), 778 (w), 761 (m), 742 (s), 995 cm⁻¹ (s); HRMS (ESI): m/z : calcd for C₁₇H₁₆NO [*M*+H⁺]: 250.1226, found: 250.1216; elemental analysis calcd (%) for C₁₇H₁₅NO (249.3): C 81.90, H 6.06, N 5.62; found: C 81.64, H 5.82, N 5.44.

(*S*)-2-(4,5-Dimethylxazol-2-yl)-1-phenylethanol [(*S*)-37**]** (Table 6, entry 4): According to GP 1, starting from *rac*-**37** (86.9 mg, 0.400 mmol, 1.00 equiv), (^{*S*}**S**)-**4a** (46.0 mg, 0.225 mmol, 0.560 equiv, 99% *ee*), CuCl (2.0 mg, 0.020 mmol, 0.050 equiv), **L1d** (13.9 mg, 0.0400 mmol, 0.100 equiv) and NaOtBu (1.9 mg, 0.020 mmol, 0.050 equiv) in toluene (4.0 mL), silyl ether (^{*S*}*R,R*)-**44a** (83 mg, 50%, d.r. 79:21) and alcohol (*S*)-**37** (36 mg, 41%, 65% *ee*) were isolated as analytically pure materials. (*S*)-**37**: $R_f = 0.25$ (cyclohexane/*tert*-butyl methyl ether 1:1); $[\alpha]_D^{20} = -19.4$ ($c = 0.530$, CHCl₃), $[\alpha]_{578}^{20} = -20.4$, $[\alpha]_{546}^{20} = -22.9$, $[\alpha]_{436}^{20} = -38.1$; HPLC

(Daicel Chiralcel AD-H, 20°C, *n*-heptane/*i*PrOH 95:5, flow rate 1.0 mL min⁻¹, $\lambda = 230$ nm): $t_R = 15.7$ min [(*S*)-**37**], 19.9 min [(*R*)-**37**]; ¹H NMR (400 MHz, CDCl₃): $\delta = 2.04$ (s, 3H), 2.19 (s, 3H), 3.02 (d, $J = 6.5$ Hz, 2H), 4.23 (brs, 1H), 5.15 (t, $J = 6.5$ Hz, 1H), 7.25–7.31 (m, 1H), 7.32–7.38 (m, 2H), 7.39–7.43 ppm (m, 2H); ¹³C NMR (100 MHz, CDCl₃): $\delta = 9.9$, 11.0, 37.6, 71.4, 125.8, 127.7, 128.5, 130.1, 142.9, 143.1, 159.9 ppm; LRMS (CI/NH₃): m/z : 218 [*M*+H⁺]; elemental analysis calcd (%) for C₁₃H₁₅NO₂ (217.3): C 71.87, H 6.96, N 6.45; found: C 71.72, H 6.98, N 6.34.

(^{*S*}S**)-1-*tert*-Butyl-1-methoxy-1-silatetraline [(^{*S*}**S**)-**52a**]**: A flame-dried Schlenk tube equipped with a magnetic stirring bar was charged with a mixture of CuCl (5.8 mg, 0.059 mmol, 0.10 equiv) and **L1d** (40.9 mg, 0.118 mmol, 0.200 equiv) under argon atmosphere. The solids were suspended in degassed, anhydrous toluene (4.0 mL). After the addition of NaOtBu (5.7 mg, 0.059 mmol, 0.10 equiv), a pale yellow solution formed within 1 min at room temperature. Subsequently, a solution of silane (^{*S*}*R,R*)-**4a** (120 mg, 0.590 mmol, 1.00 equiv) in toluene (2.0 mL) followed by dry degassed MeOH (240 μ L, 189 mg, 5.90 mmol, 10.0 equiv) were sequentially added via syringe. The resulting bright yellow solution showed gas evolution and was maintained at room temperature for 20 h, after which GLC analysis revealed approximately 80% conversion. After addition of *tert*-butyl methyl ether (10 mL) and a small portion of silica gel, the solvents were evaporated. Purification by flash column chromatography on silica gel (cyclohexane/*tert*-butyl methyl ether 97:3) afforded silyl ether (^{*S*}**S**)-**52a** (95 mg, 70%) along with unreacted silane (^{*S*}*R,R*)-**4a** (13 mg, 11%, 98% *ee*) as colorless oils. (^{*S*}**S**)-**52a**: $R_f = 0.24$ (cyclohexane/*tert*-butyl methyl ether 90:10); ¹H NMR (500 MHz, CDCl₃): $\delta = 0.95$ (ddd, $J = 15.2$, 12.4, 5.6 Hz, 1H), 0.99 (s, 9H), 1.08 (dddd, $J = 15.2$, 5.2, 4.4, 1.6 Hz, 1H), 1.76 (dddd, $J = 13.2$, 12.4, 11.4, 4.2, 2.6 Hz, 1H), 2.15 (dddd, $J = 13.3$, $J = J = 5.6$, 2.7 Hz, 1H), 2.63 (ddd, $J = 15.8$, 1.3, 2.6 Hz, 1H), 2.80 (dddd, $J = 15.6$, 6.0, $J = J = 2.0$ Hz, 1H), 3.43 (s, 3H), 7.17 (d, $J = 7.6$ Hz, 1H), 7.24 (dd, $J = J = 7.2$ Hz, 1H), 7.32 (ddd, $J = J = 7.4$, 1.3 Hz, 1H), 7.63 ppm (dd, $J = 7.2$, 1.5 Hz, 1H); ¹³C NMR (125 MHz, CDCl₃): $\delta = 8.8$, 18.5, 23.4, 26.1, 35.7, 51.4, 125.2, 128.6, 129.5, 130.9, 134.9, 150.7 ppm; IR (ATR): $\tilde{\nu} = 3055$ (w), 3001 (w), 2928 (s), 2856 (s), 2830 (m), 1591 (w), 1466 (m), 1434 (m), 1360 (w), 1293 (w), 1266 (w), 1187 (m), 1142 (m), 1077 (s), 1007 (m), 971 (m), 917 (m), 864 (w), 825 (s), 790 (s), 768 (s), 749 (s), 729 (s), 692 (s), 657 (m), 612 cm⁻¹ (s); HRMS (ESI): m/z : calcd for C₁₄H₂₂OSiNa [*M*+Na⁺]: 257.1332, found: 257.1315; elemental analysis calcd (%) for C₁₄H₂₂OSi (234.4): C 71.73, H 9.46; found: C 72.11, H 9.67.

Enantiospecific reductive cleavage of (^{*S*}S**)-**52a****: A 25 mL round-bottom flask equipped with a magnetic stirring bar, a reflux condenser and an argon-inlet was charged with a solution of (^{*S*}**S**)-**53a** (95 mg, 0.41 mmol, 1.0 equiv) in *n*-heptane (5 mL). DIBAL-H (2.0 mL, 2.0 mmol, 4.9 equiv, 1.0M in cyclohexane) was added, the reaction mixture was subsequently heated to reflux and maintained at this temperature for 12 h. The reaction was quenched at ambient temperature by careful addition of water (10 mL) followed by 2M HCl (5 mL). The mixture was extracted with *tert*-butyl methyl ether (4 \times 10 mL) and the combined organic layers were washed with brine (10 mL), dried (Na₂SO₄) and filtered. Removal of volatiles under reduced pressure followed by flash chromatography on silica gel (cyclohexane) furnished silane (^{*S*}*R,R*)-**4a** (59 mg, 71%; 49% over two steps, 97% *ee*) as a colorless oil. Analytical data agreed with those previously reported.^[20b] HPLC (Daicel Chiralcel OJ-RH, 12°C, MeCN:water = 75:25, flow rate 0.50 mL min⁻¹, $\lambda = 230$ nm): $t_R = 10.6$ min [(^{*S*}*R,R*)-**4a**], $t_R = 11.9$ min [(^{*S*}**S**)-**4a**].

Stereospecific reductive cleavage of (^{*S*}*R,R*)-7a****: A 10 mL Schlenk tube equipped with a magnetic stirring bar was charged with a solution of (^{*S*}*R,R*)-**7a** (88.5 mg, 0.220 mmol, 1.00 equiv, d.r. 86:14, \approx 96% *ee*) in CH₂Cl₂ (1.5 mL). DIBAL-H (0.44 mL, 0.44 mmol, 2.00 equiv, 1.0M in *n*-hexane) was added and the reaction mixture was subsequently maintained at ambient temperature for 24 h. The reaction was carefully quenched with *tert*-butyl methyl ether (20 mL), water (10 mL) followed by 2M HCl (5 mL) until pH 7 was reached. After separation of the organic phase, the aqueous phase was extracted with *tert*-butyl methyl ether (4 \times 10 mL). The combined organic layers were washed with brine (10 mL), dried (Na₂SO₄), filtered and, after addition of a small portion of

silica gel, volatiles were evaporated under reduced pressure. The crude product was purified by flash chromatography on silica gel with cyclohexane/*tert*-butyl methyl ether (95:5→1:1) furnishing (^{6*S*})-**4a** (44 mg, 98%, 95% *ee*) as a colorless oil and (*R*)-**6** (34 mg, 78%, 70% *ee*) as a white solid.

(S)-8-Hydroxy-8-phenyl-octane-2,6-dione [(S)-53]: To a 100 mL flask charged with (*S*)-**34** (0.500 g, 2.34 mmol, 1.00 equiv), THF (5.0 mL), absolute ethanol (0.50 mL) and liquid ammonia (65 mL) was added at -78°C sodium metal (124 mg, 5.38 mmol, 2.30 equiv). The reaction was maintained at this temperature for 1 h. Ammonia was removed under a stream of argon. To the residue was added THF (5.0 mL) and aqueous 10% H₂SO₄ (3.5 mL), and the solution was stirred at room temperature for 15 min. The reaction mixture was diluted with water (5.0 mL) and extracted with CH₂Cl₂ (3×25 mL). The organic phase was dried over MgSO₄ and the solvents were removed under reduced pressure. Purification by flash column chromatography on silica gel with cyclohexane/*tert*-butyl methyl ether (1:1) as eluent gave analytically pure (*S*)-**53** (120 mg, 22%, 69% *ee*) as a yellow oil. (*S*)-**53**: $R_f=0.18$ (cyclohexane/*tert*-butyl methyl ether 1:2); $[\alpha]_{\text{D}}^{20}=-29.4$ ($c=0.425$, CHCl₃), $[\alpha]_{\text{D}}^{20}=-31.2$, $[\alpha]_{\text{D}}^{20}=-35.0$, $[\alpha]_{\text{D}}^{20}=-60.0$, $[\alpha]_{\text{D}}^{20}=-94.8$; HPLC (Daicel Chiralpak AS-H, 20°C, *n*-heptane/*i*PrOH 90:10, flow rate 0.70 mL min⁻¹, $\lambda=230$ nm): $t_{\text{R}}=54.3$ min [(*R*)-**53**], 57.4 min [(*S*)-**53**]; ¹H NMR (400 MHz, CDCl₃): $\delta=1.83$ (quin, $J=7.1$ Hz, 2H), 2.12 (s, 3H), 2.47 (m, 4H), 2.75 (ddd, $J=17.0$, 8.0, 3.5 Hz, 1H), 2.87 (dd, $J=17.0$, 9.2 Hz, 1H), 3.62 (brs, 1H), 5.16 (dd, $J=9.2$, 3.5 Hz, 1H), 7.27–7.36 ppm (m, 5H); ¹³C NMR (100 MHz, CDCl₃): $\delta=17.3$, 29.8, 42.2, 42.4, 51.1, 69.9, 125.6, 127.6, 128.4, 143.0, 208.4, 210.4 ppm; IR (film): $\tilde{\nu}=3445$ (s), 2938 (w), 2893 (w), 1712 (s), 1695 (s), 1494 (w), 750.3 cm⁻¹ (s); HRMS (ESI⁺): m/z calcd for C₁₄H₁₈O₃Na: 257.1148; found: 257.1138 [M+Na]⁺.

Crystallographic data: Data set was collected with a Nonius KappaCCD diffractometer. Programs used: data collection COLLECT (Nonius B.V., 1998), data reduction Denzo-SMN,^[43] absorption correction Denzo,^[44] structure solution SHELXS-97,^[45] structure refinement SHELXL-97,^[46] graphics SCHAKAL.^[47]

CCDC 693437 [(^{6*S*})-*R*]-**43a**] contains the supplementary crystallographic data for this paper. These data can be obtained free of charge from The Cambridge Crystallographic Data Centre via www.ccdc.cam.ac.uk/data_request/cif

X-ray crystal structure analysis for (^{6*S*})-*R*]-43a**:** Formula C₃₀H₃₃NOSi, $M=451.66$, colorless crystal $0.25\times0.25\times0.12$ mm, $a=16.3282(7)$, $b=28.8702(12)$, $c=11.0496(4)$ Å, $\beta=92.553(2)^{\circ}$, $V=5203.6(4)$ Å³, $\rho_{\text{calcd}}=1.153$ g cm⁻³, $\mu=0.948$ mm⁻¹, empirical absorption correction ($0.798\leq T\leq 0.895$), $Z=8$, monoclinic, space group $P2_1/c$ (No. 14), $\lambda=1.54178$ Å, $T=223(2)$ K, ω and ϕ scans, 43350 reflections collected ($\pm h, \pm k, \pm l$), $[(\sin\theta)/\lambda]=0.60$ Å⁻¹, 9217 independent ($R_{\text{int}}=0.066$) and 6871 observed reflections [$I\geq 2\sigma(I)$], 601 refined parameters, $R=0.064$, $wR_2=0.164$, max. (min.) residual electron density 0.36 (−0.230) e Å⁻³, two almost identical molecules in the asymmetric unit, hydrogen atoms calculated and refined as riding atoms.

Acknowledgement

This research was funded by the Deutsche Forschungsgemeinschaft (Oe 249/4-1) and an Emmy Noether-Nachwuchsgruppe to M.O. (Oe 249/2-3 and Oe 249/2-4), as well as the Aventis Foundation (Karl-Winnacker-Stipendium to M.O., 2006–2008) and the Fonds der Chemischen Industrie (predoctoral fellowship to S.R., 2005–2007). The authors thank Gerd Fehrenbach (Universität Freiburg) for performing HPLC analyses.

- [1] a) P. G. M. Wuts, T. W. Greene, *Greene's Protective Groups in Organic Synthesis*, 4th ed., Wiley, New York, 2007, pp. 165–221; b) P. J. Kociensky, *Protecting Groups*, 3rd ed., Thieme, Stuttgart, 2004, pp. 188–230.
[2] For reviews, see: a) S. Rendler, M. Oestreich in *Modern Reduction Methods* (Eds.: P. G. Andersson, I. J. Munslow), Wiley-VCH, Wein-

heim, 2008, pp. 183–207; b) O. Riant, N. Mostefai, J. Courmarcel, *Synthesis* 2004, 2943–2958; c) T. Ohkuma, R. Noyori in *Comprehensive Asymmetric Catalysis—Supplement 1* (Eds.: E. N. Jacobsen, A. Pfaltz, H. Yamamoto), Springer, Berlin, 2004, pp. 55–71; d) H. Nishiyama in *Comprehensive Asymmetric Catalysis, Vol. 1* (Eds.: E. N. Jacobsen, A. Pfaltz, H. Yamamoto), Springer, Berlin, 1999, pp. 267–288.

- [3] T. Isobe, K. Fukuda, Y. Araki, T. Ishikawa, *Chem. Commun.* 2001, 243–244.
[4] For a brief summary, see: S. Rendler, M. Oestreich, *Angew. Chem.* 2008, 120, 254–257; *Angew. Chem. Int. Ed.* 2008, 47, 248–250.
[5] a) Cu–H-catalyzed silylation of secondary alcohols: S. Rendler, G. Auer, M. Oestreich, *Angew. Chem.* 2005, 117, 7793–7797; *Angew. Chem. Int. Ed.* 2005, 44, 7620–7624; b) Cu–H-catalyzed silylation of tertiary alcohols: B. Karatas, S. Rendler, R. Fröhlich, M. Oestreich, *Org. Biomol. Chem.* 2008, 6, 1435–1440; c) Rh–H-catalyzed silylation of secondary alcohols: H. F. T. Klare, M. Oestreich, *Angew. Chem.* 2007, 119, 9496–9499; *Angew. Chem. Int. Ed.* 2007, 46, 9335–9338.
[6] a) Catalyst-controlled silylation of *meso* diols: Y. Zhao, J. Rodrigo, A. H. Hoveyda, M. L. Snapper, *Nature* 2006, 443, 67–70; b) catalyst-controlled kinetic resolution of racemic diols: Y. Zhao, A. W. Mitra, A. H. Hoveyda, M. L. Snapper, *Angew. Chem.* 2007, 119, 8623–8626; *Angew. Chem. Int. Ed.* 2007, 46, 8471–8474.
[7] a) E. Vedejs, M. Jure, *Angew. Chem.* 2005, 117, 4040–4069; *Angew. Chem. Int. Ed.* 2005, 44, 3974–4001; b) H. B. Kagan, J. C. Fiaud, *Top. Stereochem.* 1988, 18, 249–330.
[8] a) T. Rovis in *New Frontiers in Asymmetric Catalysis* (Eds.: K. Mikami, M. Lautens), Wiley, New York, 2007, pp. 275–311; b) M. C. Willis, *J. Chem. Soc. Perkin Trans. 1* 1999, 1765–1784.
[9] E. J. Jarvo, S. J. Miller in *Comprehensive Asymmetric Catalysis—Supplement 1* (Eds.: E. N. Jacobsen, A. Pfaltz, H. Yamamoto), Springer, Berlin, 2004, pp. 189–206.
[10] a) J. Y. Corey, *Adv. Silicon Chem.* 1991, 1, 327–387; b) E. Lukevics, M. Dzintara, *J. Organomet. Chem.* 1985, 295, 265–315.
[11] Selected recent examples: a) Pd/C and Rh^{II}: C. N. Scott, C. S. Wilcox, *Synthesis* 2004, 2273–2276; b) Ru^I: R. L. Miller, S. V. Mairfeld, D. Lee, *Org. Lett.* 2004, 6, 2773–2776; c) Cu^I: H. Ito, A. Watanabe, M. Sawamura, *Org. Lett.* 2005, 7, 1869–1871; d) Au^I: H. Ito, K. Takagi, T. Miyahara, M. Sawamura, *Org. Lett.* 2005, 7, 3001–3004; e) Cu^{II}: Y. Gunji, Y. Yamashita, T. Ikeno, T. Yamada, *Chem. Lett.* 2006, 714–715.
[12] Review on the related Cu–H-catalyzed carbonyl reduction: S. Rendler, M. Oestreich, *Angew. Chem.* 2007, 119, 504–510; *Angew. Chem. Int. Ed.* 2007, 46, 498–504.
[13] C. Lorenz, U. Schubert, *Chem. Ber.* 1995, 128, 1267–1269.
[14] A closely related σ -bond metathesis has been suggested earlier: D. H. Appella, Y. Moritani, R. Shintani, E. M. Ferreira, S. L. Buchwald, *J. Am. Chem. Soc.* 1999, 121, 9473–9474.
[15] a) M. Oestreich, *Chem. Eur. J.* 2006, 12, 30–37; b) M. Oestreich, *Synlett* 2007, 1629–1643.
[16] a) M. Oestreich, S. Rendler, *Angew. Chem.* 2005, 117, 1688–1691; *Angew. Chem. Int. Ed.* 2005, 44, 1661–1664; b) S. Rendler, M. Oestreich, C. P. Butts, G. C. Lloyd-Jones, *J. Am. Chem. Soc.* 2007, 129, 502–503; c) S. Rendler, M. Oestreich, *Beilstein J. Org. Chem.* 2007, 3, 9; d) S. Rendler, R. Fröhlich, M. Keller, M. Oestreich, *Eur. J. Org. Chem.* 2008, 2582–2591.
[17] a) L. H. Sommer, *Stereochemistry, Mechanism, and Silicon*, McGraw-Hill, New York, 1965; b) L. H. Sommer, *Intra-Sci. Chem. Rep.* 1973, 7, 1–44; c) R. J. P. Corriu, C. Guérin, J. J. E. Moreau, *Top. Stereochem.* 1984, 15, 43–198.
[18] a) L. H. Sommer, C. L. Frye, *J. Am. Chem. Soc.* 1959, 81, 1013; b) L. H. Sommer, C. L. Frye, G. A. Parker, K. W. Michael, *J. Am. Chem. Soc.* 1964, 86, 3271–3279.
[19] a) G. Bertrand, J. Dubac, P. Mazerolles, J. Ancelle, *Nouv. J. Chim.* 1982, 6, 381–386; b) G. L. Larson, E. Torres, *J. Organomet. Chem.* 1985, 293, 19–27; c) P. Jankowski, E. Schaumann, J. Wicha, A. Zarecki, G. Adiwidjaja, *Tetrahedron: Asymmetry* 1999, 10, 519–526;

- d) P. Jankowski, E. Schaumann, J. Wicha, A. Zarecki, G. Adiwidjaja, M. Asztemborska, *Chem. Commun.* **2000**, 1029–1030.
- [20] a) M. Oestreich, U. K. Schmid, G. Auer, M. Keller, *Synthesis* **2003**, 2725–2739; b) S. Rendler, G. Auer, M. Keller, M. Oestreich, *Adv. Synth. Catal.* **2006**, *348*, 1171–1182.
- [21] D. R. Schmidt, S. J. O'Malley, J. L. Leighton, *J. Am. Chem. Soc.* **2003**, *125*, 1190–1191.
- [22] It must be noted that this correlation only holds true if both reactions—with racemic as well as enantiopure silane—follow identical kinetics.
- [23] Synthesis and resolution of 1-silaindane **5a** was conducted analogous to a previously reported procedure.^[20b] see Supporting Information for details.
- [24] a) S. E. Denmark, R. T. Jacobs, G. Dai-Ho, S. Wilson, *Organometallics* **1990**, *9*, 3015–3019; b) A. G. Myers, S. E. Kephart, H. Chen, *J. Am. Chem. Soc.* **1992**, *114*, 7922–7923; c) S. E. Denmark, B. D. Griedel, D. M. Coe, *J. Org. Chem.* **1993**, *58*, 988–990; d) K. Matsumoto, K. Oshima, K. Utimoto, *J. Org. Chem.* **1994**, *59*, 7152–7155; e) X. Zhang, K. N. Houk, J. L. Leighton, *Angew. Chem.* **2005**, *117*, 960–963; *Angew. Chem. Int. Ed.* **2005**, *44*, 938–941.
- [25] In this reversed scenario for kinetic resolution, racemic silane *rac-4a* (1.0 equiv) was subjected to Cu–H-catalyzed dehydrogenative Si–O coupling using an enantiopure pyridyl alcohol (0.50 equiv).^[20b]
- [26] J. F. Daeuble, C. McGettigan, J. M. Stryker, *Tetrahedron Lett.* **1990**, *31*, 2397–2400.
- [27] T. O. Luukas, C. Girard, D. R. Fenwick, H. B. Kagan, *J. Am. Chem. Soc.* **1999**, *121*, 9299–9306.
- [28] In our hands, the determination of conversion by ¹H NMR spectroscopy from the crude reaction mixture emerged as a critical point. The deviation from the given values is about ±3% and might account for occasional inconsistencies in Tables 4–7.
- [29] Reductive cleavage of silyl ethers proceeds under retention of configuration at silicon: M. Oestreich, G. Auer, M. Keller, *Eur. J. Org. Chem.* **2005**, 184–195.
- [30] C. Yu, O. Meth-Cohn, *Tetrahedron Lett.* **1999**, *40*, 6665–6668.
- [31] Selected examples for enzymatic kinetic resolutions of pyridyl methanols: a) By oxidation: M. Takemoto, K. Achiwa, *Tetrahedron: Asymmetry* **1995**, *6*, 2925–2928; b) by acylation: J. Uenishi, T. Hiraoaka, S. Hata, K. Nishikawa, O. Yonemitsu, K. Nakamura, H. Tsukube, *J. Org. Chem.* **1998**, *63*, 2481–2487.
- [32] C. Mazet, S. Roseblade, V. Köhler, A. Pfaltz, *Org. Lett.* **2006**, *8*, 1879–1882.
- [33] S. Danishefsky, A. Zimmer, *J. Org. Chem.* **1976**, *41*, 4059–4064.
- [34] TURBOMOLE (Ver. 5.9); University of Karlsruhe, **2006** (<http://www.turbomole.com>).
- [35] J. P. Perdew, K. Burke, M. Ernzerhof, *Phys. Rev. Lett.* **1996**, *77*, 3865–3868.
- [36] a) A. D. Becke, *J. Chem. Phys.* **1993**, *98*, 5648–5652; b) P. J. Stephens, F. J. Devlin, C. F. Chabalowski, M. J. Frisch, *J. Phys. Chem.* **1994**, *98*, 11623–11627.
- [37] S. Grimme, *J. Chem. Phys.* **2003**, *118*, 9095–9102.
- [38] A. Schäfer, C. Huber, R. Ahlrichs, *J. Chem. Phys.* **1994**, *100*, 5829–5835. For TZVPP, additional functions of higher angular momentum are added. Contradictions: Cu: [6s4p3d1f], P: [5s5p2d1f], O: [5s3p2d1f], H: [3s2p1d], C: [5s3p2d1f], Si: [5s5p2d1f] (basis set from ftp.chemie.uni-karlsruhe.de/pub/).
- [39] S. Díez-González, E. D. Stevens, N. M. Scott, J. L. Petersen, S. P. Nolan, *Chem. Eur. J.* **2008**, *14*, 158–168.
- [40] a) H. Brunner, W. Michling, *J. Organomet. Chem.* **1984**, *275*, C17–C21; b) J. M. Stryker, D. M. Bestrensky in *Catalysis of Organic Reactions* (Ed.: W. E. Pascoe), Marcel Dekker, New York, **1992**, pp. 29–44.
- [41] a) **L1b**: T. Allman, R. G. Goel, *Can. J. Chem.* **1982**, *60*, 716–722; b) **L1c**, **L1e**: H. A. Brune, M. Falck, R. Hemmer, G. Schmidtberg, H. G. Alt, *Chem. Ber.* **1984**, *117*, 2791–2802; c) **L1d**: G. P. Schiemenz, K. Röhlk, *Chem. Ber.* **1971**, *104*, 1219–1233; d) **L1f**: J. Porwisiak, M. Schlosser, *Chem. Ber.* **1996**, *129*, 233–235.
- [42] L. Jafarpour, E. D. Stevens, S. P. Nolan, *J. Organomet. Chem.* **2000**, *606*, 49–54.
- [43] Z. Otwinowski, W. Minor, *Methods Enzymol.* **1997**, *276*, 307–326.
- [44] Z. Otwinowski, D. Borek, W. Majewski, W. Minor, *Acta Crystallogr. Sect. A* **2003**, *59*, 228–234.
- [45] G. M. Sheldrick, *Acta Crystallogr. Sect. A* **1990**, *46*, 467–473.
- [46] G. M. Sheldrick, *Acta Crystallogr. Sect. A* **2008**, *64*, 112–122.
- [47] E. Keller, *SCHAKAL*, University of Freiburg (Germany), **1997**.

Received: July 7, 2008

Published online: November 19, 2008